

TP
1536
c.1

NASA Technical Paper 1536

LOAN COPY RETURN TO
AFWL TECHNICAL LIBRARY
KIRTLAND AFB, N. M.



Inclusion of Unsteady Aerodynamics in Longitudinal Parameter Estimation From Flight Data

M. J. Queijo, William R. Wells,
and Dinesh A. Keskar

DECEMBER 1979





NASA Technical Paper 1536

Inclusion of Unsteady Aerodynamics in Longitudinal Parameter Estimation From Flight Data

M. J. Queijo
*Langley Research Center
Hampton, Virginia*

William R. Wells
*Wright State University
Dayton, Ohio*

Dinesh A. Keskar
*SDC Integrated Services, Inc.
Hampton, Virginia*

NASA

National Aeronautics
and Space Administration

**Scientific and Technical
Information Branch**

1979

SUMMARY

A simple vortex system is used to model unsteady aerodynamic effects into the rigid-body longitudinal equations of motion of an aircraft. With the formulation used, only steady-state aerodynamic derivatives appear in the equations. It is found expedient to transform the equations into the frequency domain to make them useful for extracting aerodynamic parameters from flight data. The equations are used in the development of a parameter-extraction algorithm. If the algorithm is used with the unsteady aerodynamic modeling included, all extracted aerodynamic derivatives are the steady-state derivatives. If unsteady aerodynamic modeling is omitted, some extracted parameters will include the effects of unsteady aerodynamics and are interpreted as combinations of steady-state and acceleration parameters. Use of the two parameter-estimation modes, one including and the other omitting unsteady-aerodynamic modeling, provides a means of estimating some acceleration derivatives. Computer-generated data and flight data are used to demonstrate the use of the parameter-extraction algorithm.

INTRODUCTION

Extraction of aerodynamic parameters from flight data has become a routine task for numerous organizations. Sophisticated mathematical techniques have been developed for this purpose. Although parameter-extraction methods have been well developed and work very well with computer-generated data, several problems generally become apparent when applied to flight data. Some problems documented in reference 1 include:

- (1) Extraction of different numerical values for the same parameter, under similar flight conditions
- (2) Estimated variance in parameters which are much too optimistic when compared to values from ensemble averages
- (3) Dependence of values of extracted parameters on the shape of the control input

One possibility that could have impact on these items is that unsteady aerodynamics associated with load buildup following an increase in angle of attack generally has not been included in parameter-estimation algorithms. Another possibility is that unsteady aerodynamics associated with downwash at the horizontal tail is generally approximated by assuming the existence of certain acceleration derivatives, in particular the acceleration derivative $C_{m\dot{\alpha}}$. In the present study, the idea is that better consistency in extracted parameters might be obtained if the two unsteady aerodynamic effects are modeled more precisely.

Although various methods were available for calculating unsteady aerodynamic loads on lifting surfaces (e.g., refs. 2 to 4), they were generally too complex for use in equations of motion or for parameter identification purposes. The study of reference 5 was a preliminary attempt to develop a method for including unsteady effects in equations of motion that could be used in parameter identification. In reference 5 a simple vortex system was developed for estimating indicial lift and downwash associated with circulation for unswept wings in incompressible flow. This system gave results that were in good agreement with more accurate and complex vortex systems. The vortex system was generalized in reference 6, and the results were extended to obtain indicial lift for tapered, swept wings in incompressible flow.

The purposes of the present study were as follows: (1) To develop further the methods of references 5 and 6 to derive equations for the downwash behind tapered, swept wings; (2) to develop equations of motion including unsteady aerodynamic effects; (3) to develop algorithms for parameter extraction accounting for unsteady effects; and (4) to apply the algorithms to flight data.

SYMBOLS

All aerodynamic coefficients are based on wing geometry.

a_z	vertical acceleration, g units
A	aspect ratio, b^2/S
A_{ij}	elements of matrix
b	span, m
c	chord, m
\bar{c}	average chord, m
C_L	lift coefficient, $\frac{\text{Lift}}{\bar{q}S_w}$
$\tilde{C}_{L_{t_1}}, \tilde{C}_{L_{t_2}}, \tilde{D}$	parameters defined in equations (28), (29), and (30)
C_m	pitching-moment coefficient, $\frac{\text{Pitching moment}}{\bar{q}S_w c_w}$, about aircraft center of gravity
$E_i(\)$	exponential integral of variable (), $\int_{-\infty}^x \frac{e^v}{v} dv$
f_1, f_2, f_3	downwash factors
F, G, H	coefficients used in modeling downwash when indicial lift function is neglected
g	acceleration due to gravity, 9.8 m/sec^2

i	$= \sqrt{-1}$
I_Y	moment of inertia about Y-axis, $\text{kg}\cdot\text{m}^2$
l	distance behind wing root quarter-chord point, m
l_t	distance from aircraft center of gravity to aerodynamic center of horizontal tail, m
m	aircraft mass, kg
N	number of points
\dot{q}	pitch rate, deg/sec
\bar{q}	dynamic pressure, $\frac{1}{2} \rho u^2 S$, N/m^2
R	noise covariance matrix
S	area, m^2
t, τ	time, sec
u	velocity, m/sec
v	dummy variable
w	downwash velocity
\bar{x}	distance downstream from aircraft center of gravity to wing aerodynamic center, m
y, z	constants in indicial lift function
α	geometric angle of attack, deg or rad
Γ	circulation strength, m^2/sec
δ	deflection, deg or rad
$\Delta C_L(t)$	lift due to unit step in α
$\Delta \varepsilon(t)$	response in downwash to unit step in α , deg or rad
ε	downwash angle, deg or rad
θ	parameter vector
λ	taper ratio, c_t/c_r
Λ	sweep of quarter-chord line, positive for sweepback, deg or rad

ρ air density, kg/m³

ω frequency, rad/sec

$$C_{L\alpha} = \frac{\partial C_L}{\partial \alpha}$$

$$C_{L\delta_e} = \frac{\partial C_L}{\partial \delta_e}$$

$$C_{m\dot{\alpha}} = \frac{\partial C_m}{\partial \frac{\dot{\alpha} \bar{c}_w}{2u}}$$

$$C_{Lq} = \frac{\partial C_L}{\partial \frac{q \bar{c}_w}{2u}}$$

$$C_{m\alpha} = \frac{\partial C_m}{\partial \alpha}$$

$$C_{m\delta_e} = \frac{\partial C_m}{\partial \delta_e}$$

$$C_{mq} = \frac{\partial C_m}{\partial \frac{q \bar{c}_w}{2u}}$$

$$C_{mq}' = (C_{mq})_{ss} + C_{m\dot{\alpha}}$$

$$C_{m\alpha}' = (C_{m\alpha})_{ss} - \frac{\rho S_w \bar{c}_w}{4m} (C_{L\alpha})_{ss} C_{m\dot{\alpha}}$$

$$C_{m\delta_e}' = (C_{m\delta_e})_{ss} - \frac{\rho S_w \bar{c}_w}{4m} C_{L\delta_e} C_{m\dot{\alpha}}$$

Subscripts:

e elevator

E effective

f fuselage

k variable index

l quantity at distance l

r root

s unsteady aerodynamics only in downwash

ss steady state (no unsteady aerodynamic effects)

t horizontal tail or wing tip

w wing

Superscripts:

~ variable in frequency domain

' coefficient used in modeling downwash when indicial lift function is included

· derivative with respect to time

Abbreviations:

det	determinant
diag	diagonal
mag	magnitude
Re	real part

ANALYSIS

The longitudinal aerodynamic parameters of an aircraft are determined primarily by the lift forces on the wing, horizontal tail, and elevator. In unsteady motion, the forces can be considered to be composed of three parts (ref. 7). One part is due to circulatory flow associated with angle-of-attack variation where this variation is caused by the vertical (plunging) motion of the aerodynamic center. A second part is associated with circulatory flow and ascribed to the curvature of the flow streamlines relative to the surface when the surface is performing a pitching motion. This second component is often analyzed by considering an equivalent system which replaces the airfoil and circular streamlines with a circular-arc airfoil in rectilinear flow. The effective angle of attack associated with the curvature is the difference in surface slope between the quarter-chord and three-quarter-chord points. This effective angle of attack associated with rotation can be included with the angle of attack due to vertical motion for purposes of analysis (ref. 7). A third part is due to instantaneous acceleration of noncirculatory potential flow. This lift is equal to the product of the virtual additional mass of the moving surface and the acceleration normal to the surface. This effect is generally small and is not considered in this paper. However, the effect could be important for very lightweight aircraft.

Lift Due to Circulatory Flow

The instantaneous lift on an airfoil associated with circulatory flow is obtained by use of an indicial lift function and the effective angle of attack. The indicial lift function $\Delta C_L(t)$ is the lift response due to a unit step increment in the effective angle of attack. The analysis of reference 6 resulted in a general expression for indicial lift associated with vertical motion, which could be fitted accurately by an exponential equation of the form

$$\Delta C_L(t) = (C_{L\alpha})_{SS} \left(1 - ye^{-\frac{zut}{c_r/2}} \right) \quad (1)$$

The constants y and z are functions of wing (or tail) geometry and are given in reference 6 for a wide range of wing geometries. The lift for arbitrary variation in angle of attack can be obtained by using equation (1) in Duhamel's integral as

$$C_L(t) = \int_0^t \Delta C_L(t - \tau) \dot{\alpha}_E(\tau) d\tau \quad (2)$$

Application of equation (2) requires that the effective angle of attack be determined for a surface performing a plunging and/or pitching motion. The next two sections are concerned with determining the effective angle of attack for a wing and a horizontal tail surface.

Effective Angle of Attack of Wing

The flow around the wing and hence the wake produced by the wing are assumed to be uninfluenced by the presence of the horizontal tail. The effective angle of attack of the wing can be considered to be associated with the flow normal to the wing at the quarter-chord point plus the curvature effect (mentioned previously) associated with pitching motion. The effective angle of attack can be shown to be

$$(\alpha_E)_w = \alpha + q \frac{\bar{x}}{u} + \frac{q\bar{c}_w}{2u} \quad (3)$$

where the last term is the curvature effect. The last two terms can be combined to yield

$$(\alpha_E)_w = \alpha + \frac{q}{u} \left(\bar{x} + \frac{\bar{c}_w}{2} \right) \quad (4)$$

Effective Angle of Attack of Horizontal Tail

The effective angle of attack of the horizontal tail involves the same factors as that of the wing, but it is also influenced by the downwash from the wing. The effective angle of attack of the horizontal tail, therefore, is

$$(\alpha_E)_t = \alpha + \frac{q}{u} \left(l_t + \frac{\bar{c}_t}{2} \right) - (\epsilon_l)_t \quad (5)$$

The approach used in determining downwash for arbitrary variation in angle of attack is to first calculate the downwash caused by a unit step increase in wing angle of attack, and then to use Duhamel's integral to obtain downwash for arbitrary variation in wing angle of attack.

The simple vortex system illustrated in figure 1 and used in reference 6 is used to calculate downwash. The system consists of a bound vortex along the wing quarter-chord line, a trailing vortex at each wing tip, and a shed vortex connecting the downstream ends of the trailing vortices. The vortices are all in a plane parallel to the free-stream direction, and the trailing vortices remain parallel to the free-stream direction. The vortex system stretches in the downstream direction at one-half of the free-stream velocity. A discussion

and justification for use of this vortex system to represent a complex physical situation is given in reference 6. The vortex strength is the same in all portions of the system. The time variation of the lift following a unit step increase in angle of attack and, consequently, the corresponding circulation strength are determined by equation (1).

In keeping with the simple vortex representation used, downwash is calculated only in the plane of the vortex system, midway between the two trailing vortices. The downwash at a distance l downstream from the midpoint of the bound vortex can be determined by use of the Biot-Savart law (ref. 8) and is

$$w_l(t) = \frac{\Gamma}{\pi c_r} [f_1 + f_2(t) + f_3(t)] \quad (6)$$

where

$$\begin{aligned}
 f_1 &= \frac{c_r}{2l} \left\{ \tan \Lambda + \frac{\left[\frac{A(1+\lambda)}{4} \right] \sec^2 \Lambda - \frac{l}{c_r} \tan \Lambda}{\sqrt{\left[\frac{A(1+\lambda)}{4 \cos \Lambda} - \frac{l}{c_r} \sin \Lambda \right]^2 + \left(\frac{l}{c_r} \cos \Lambda \right)^2}} \right\} \\
 f_2(t) &= \frac{2}{A(1+\lambda)} \left\{ \frac{\frac{l}{c_r} - \frac{A(1+\lambda)}{4} \tan \Lambda}{\sqrt{\left[\frac{l}{c_r} - \frac{A(1+\lambda)}{4} \tan \Lambda \right]^2 + \left[\frac{A(1+\lambda)}{4} \right]^2}} \right. \\
 &\quad \left. - \frac{\frac{l}{c_r} - 1 - \frac{ut}{2c_r} - \frac{A(1+\lambda)}{4} \tan \Lambda}{\sqrt{\left[\frac{l}{c_r} - 1 - \frac{ut}{2c_r} - \frac{A(1+\lambda)}{4} \tan \Lambda \right]^2 + \left[\frac{A(1+\lambda)}{4} \right]^2}} \right\} \\
 f_3(t) &= - \frac{1}{2 \left(\frac{l}{c_r} - 1 - \frac{ut}{2c_r} \right)} \left\{ \tan \Lambda \right. \\
 &\quad \left. + \frac{\frac{A(1+\lambda)}{4} \sec^2 \Lambda - \left(\frac{l}{c_r} - 1 - \frac{ut}{2c_r} \right) \tan \Lambda}{\sqrt{\left[\frac{A(1+\lambda)}{4 \cos \Lambda} - \left(\frac{l}{c_r} - 1 - \frac{ut}{2c_r} \right) \sin \Lambda \right]^2 + \left[\left(\frac{l}{c_r} - 1 - \frac{ut}{2c_r} \right) \cos \Lambda \right]^2}} \right\}
 \end{aligned} \quad (7)$$

In equations (7), f_1 is associated with the quarter-chord-line bound vortex, $f_2(t)$ is associated with the two wing-tip vortices, and $f_3(t)$ is associated with the shed vortex. In deriving equations (7), use was made of the geometric relationship

$$\frac{b}{c_r} = \frac{A(1 + \lambda)}{2}$$

The Kutta-Joukowski equation used to relate lift to circulation is

$$L(t) = \rho u b \Gamma(t)$$

Solving for $\Gamma(t)$ and substituting into equation (6) results in

$$w_\lambda(t) = \frac{L(t)}{\pi \rho u b c_r} [f_1 + f_2(t) + f_3(t)] \quad (8)$$

The downwash angle is defined as

$$\epsilon_\lambda(t) = \frac{w_\lambda(t)}{u}$$

hence, equation (8) can be written as

$$\epsilon_\lambda(t) = \frac{L(t)}{\pi \rho u^2 b c_r} [f_1 + f_2(t) + f_3(t)]$$

Since the area of a wing is given by $S = b\bar{c} = b c_r \frac{1 + \lambda}{2}$, the downwash equation can be written as

$$\epsilon_\lambda(t) = \frac{1 + \lambda}{4\pi} C_L(t) [f_1 + f_2(t) + f_3(t)]$$

The downwash following a unit step increase in angle of attack, therefore, is

$$\Delta \epsilon_\lambda(t) = \frac{1 + \lambda}{4\pi} \Delta C_L(t) [f_1 + f_2(t) + f_3(t)] \quad (9)$$

Substituting equation (1) into equation (9) results in

$$\Delta \epsilon_\lambda(t) = \frac{1 + \lambda}{4\pi} (C_{L\alpha})_{ss} \left(1 - ye^{-\frac{-z}{c_r/2} ut} \right) [f_1 + f_2(t) + f_3(t)] \quad (10)$$

The vortex system being used is a simple model for a complex physical system; therefore, equation (10) is not expected to be very accurate quantitatively. However, the functional relationship between downwash and time should be useful. A means of improving the accuracy of equation (10) is to assure correctness of the equation at known conditions. In the case of downwash, there are reasonably accurate methods of computing downwash under steady-state conditions. Under such conditions equation (10) becomes

$$(\Delta \epsilon_l)_{ss} = \frac{1 + \lambda}{4\pi} (C_{L\alpha})_{ss} [f_1 + f_2(\infty) + f_3(\infty)] \quad (11)$$

Dividing equation (10) by equation (11) results in

$$\Delta \epsilon_l(t) = (\Delta \epsilon_l)_{ss} \left(1 - ye^{-z \frac{ut}{c_r/2}} \right) \left[\frac{f_1 + f_2(t) + f_3(t)}{f_1 + f_2(\infty) + f_3(\infty)} \right] \quad (12)$$

However, $(\Delta \epsilon_l)_{ss} = \left(\frac{\partial \epsilon}{\partial \alpha} \right)_{l,ss}$. Therefore equation (12) becomes

$$\Delta \epsilon_l(t) = \left(\frac{\partial \epsilon}{\partial \alpha} \right)_{l,ss} \left(1 - ye^{-z \frac{ut}{c_r/2}} \right) \left[\frac{f_1 + f_2(t) + f_3(t)}{f_1 + f_2(\infty) + f_3(\infty)} \right] \quad (13)$$

The terms $f_2(\infty)$ and $f_3(\infty)$ can be evaluated by letting $t \rightarrow \infty$ in equations (7). The results are

$$f_2(\infty) = \frac{2}{A(1 + \lambda)} \left\{ \frac{\frac{l}{c_r} - \frac{A(1 + \lambda)}{4} \tan \Lambda}{\sqrt{\left[\frac{l}{c_r} - \frac{A(1 + \lambda)}{4} \tan \Lambda \right]^2 + \left[\frac{A(1 + \lambda)}{4} \right]^2}} + 1 \right\} \quad (14)$$

$$f_3(\infty) = 0$$

Equation (13) is complicated because of the long expressions for $f_1(t)$, $f_2(t)$, $f_3(t)$, and $f_2(\infty)$ as given by equations (7) and (14). After computing downwash for a few specific cases and some experimentation, it was found (as in ref. 5) that equation (13) could be approximated very closely by the equation

$$\Delta \varepsilon_l(t) = \left(\frac{\partial \varepsilon}{\partial \alpha} \right)_{l,ss} \left[1 - \frac{F'}{\left(\frac{l}{c_r} - 1 \right) - \frac{ut}{2c_r}} - G'e^{-H' \frac{ut}{c_r/2}} \right] \quad (15)$$

Equation (15) is also in a convenient form to use in frequency-response calculations, as discussed subsequently, because Fourier transforms are available for the terms involved. Transforms are not known to exist for some terms of the downwash expression given as equation (10). Values of F' , G' , and H' are functions of wing geometry and length l and can be determined by curve fitting equation (15) to results calculated from equation (13). Details of this procedure are given in appendix A.

Lift on Wing

The lift associated with circulation for arbitrary variation in angle of attack of a wing (uninfluenced by the tail) is obtained by use of equations (1), (2), and (4) and is

$$C_{L_w}(t) = (C_{L\alpha})_{w,ss} \int_0^t \left[1 - y_w e^{-z_w \frac{u(t-\tau)}{c_{rw}/2}} \right] \left[\dot{\alpha}(\tau) + \left(\bar{x} + \frac{\bar{c}_w}{2} \right) \frac{\dot{q}(\tau)}{u} \right] d\tau \quad (16)$$

Lift on Horizontal Tail

The lift associated with circulatory flow of the horizontal tail is obtained by use of equations (1), (2), and (5) and is

$$C_{L_t}(t) = (C_{L\alpha})_{t,ss} \int_0^t \left[1 - y_t e^{-z_t \frac{u(t-\tau)}{c_{rt}/2}} \right] \left[\dot{\alpha}(\tau) + \left(l_t + \frac{\bar{c}_t}{2} \right) \frac{\dot{q}(\tau)}{u} - \dot{\varepsilon}_l(\tau) \right] d\tau \quad (17)$$

The downwash for arbitrary angle of attack required in equation (17) is obtained by use of equation (15) in Duhamel's integral and is

$$\varepsilon_l(t) = \left(\frac{\partial \varepsilon}{\partial \alpha} \right)_{l,ss} \int_0^t \left[1 - \frac{F'_w}{\left(\frac{l}{c_{rw}} - 1 \right) - \frac{u(t-\tau)}{2c_{rw}}} - G'_w e^{-H'_w \frac{u(t-\tau)}{c_{rw}/2}} \right] \dot{\alpha}(\tau) d\tau \quad (18)$$

Lift Due to Elevator Deflection

In order to determine the lift associated with arbitrary variation of elevator deflection, an indicial response function must be obtained to use in Duhamel's integral. The lift would then be given by an equation of the form

$$C_{L_e}(t) = \int_0^t \Delta C_{L_e}(t - \tau) \dot{\delta}_e(\tau) d\tau \quad (19)$$

where $\Delta C_{L_e}(t)$ is the indicial function, that is, the time variation of lift associated with a unit step in elevator deflection. No data or convenient theory for obtaining ΔC_{L_e} were found to serve as a guide for developing a simple expression as would be required in parameter identification. However, on the basis of the wing indicial lift function, a control-surface indicial response might have the form

$$\Delta C_{L_e} = \left(C_{L_{\delta_e}} \right)_{ss} \left(1 - y_e e^{-z_e \frac{ut}{\bar{c}_e/2}} \right) \quad (20)$$

The lift for arbitrary variation in control deflection would be given by using equation (20) in Duhamel's integral.

EQUATIONS OF MOTION

Unsteady Aerodynamics in Downwash

Indicial lift function.- By assuming that initial pitch attitude and its variations are small, the rigid-body longitudinal perturbation equations of motion are

$$\dot{\alpha}(t) = q(t) - \frac{\rho u S_w}{2m} C_L(t) \quad (21)$$

and

$$\dot{q}(t) = \frac{\rho u^2 S_w \bar{c}_w}{2I_Y} C_m(t) \quad (22)$$

The unsteady aerodynamic effects are modeled in the terms $C_L(t)$ and $C_m(t)$, which are expressed as

$$C_L(t) = C_{L_w}(t) + C_{L_t}(t) + C_{L_e}(t) \quad (23)$$

and

$$C_m(t) = -\frac{l_t}{\bar{c}_w} \left[C_{L_t}(t) + C_{L_e}(t) \right] + (C_{m\alpha})_f \alpha - \frac{\bar{x}}{\bar{c}_w} C_{L_w}(t) \quad (24)$$

(All coefficients are based on wing geometry.)

When equations (16), (17), (18), and (19) are substituted into equations (23) and (24) and the results are used in equations (21) and (22), the consequence is a pair of integro-differential equations involving convolution integrals. The solution of the equations is very time consuming even on a high-speed digital computer. Computation of sensitivity coefficients, which is an integral part of several parameter-extraction techniques, becomes very cumbersome. The equations, therefore, are transformed to the frequency domain to simplify them and make them more practical for use in parameter extraction.

The equations of motion in the frequency domain can be shown to be

$$i\omega\tilde{\alpha} = \tilde{q} - \frac{\rho u S_w}{2m} \left\{ \left(\tilde{C}_{L_w} + \tilde{C}_{L_{t_1}} \right) \tilde{\alpha} + \left[\left(\bar{x} + \frac{\bar{c}_w}{2} \right) \tilde{C}_{L_w} + \left(l_t + \frac{c_t}{2} \right) \tilde{C}_{L_{t_2}} \right] \frac{\tilde{q}}{u} + \tilde{C}_{L_e} \tilde{\delta}_e \right\} \quad (25)$$

and

$$i\omega\tilde{q} = -\frac{\rho u^2 S_w \bar{c}_w}{2I_y} \left\{ \left(\frac{\bar{x}}{\bar{c}_w} \tilde{C}_{L_w} + \frac{l_t}{\bar{c}_w} \tilde{C}_{L_{t_1}} \right) \tilde{\alpha} + \left[\left(\bar{x} + \frac{\bar{c}_w}{2} \right) \frac{\bar{x}}{\bar{c}_w} \tilde{C}_{L_w} + \left(l_t + \frac{\bar{c}_t}{2} \right) \frac{l_t}{\bar{c}_w} \tilde{C}_{L_{t_2}} \right] \frac{\tilde{q}}{u} + \frac{l_t}{\bar{c}_w} \tilde{C}_{L_e} \tilde{\delta}_e - \left(\tilde{C}_{m\alpha} \right)_f \tilde{\alpha} \right\} \quad (26)$$

where

$$\tilde{C}_{L_w} = (C_{L\alpha})_{w,ss} \left(1 - \frac{i\omega y_w}{i\omega + \frac{z_w u}{c_{r_w}/2}} \right) \quad (27)$$

$$\tilde{C}_{L_{t_1}} = (C_{L\alpha})_{t,ss} \left(1 - \frac{i\omega y_t}{i\omega + \frac{z_t u}{c_{r_t}/2}} \right) \left\{ \left[1 - \left(\frac{\partial \epsilon}{\partial \alpha} \right)_{l,ss} \right] + \left(\frac{\partial \epsilon}{\partial \alpha} \right)_{l,ss} \tilde{D} \right\} \quad (28)$$

$$\tilde{D} = \left[\frac{2i\omega F'_w}{u/c_{r_w}} e^{-\left(2 \frac{\lambda - c_{r_w}}{u}\right) i\omega} \right] \left[E_i \left(2 \frac{\lambda - c_{r_w}}{u} i\omega \right) \right] + \frac{i\omega G'_w}{i\omega + \frac{H'_w u}{c_{r_w}/2}} \quad (29)$$

$$\tilde{C}_{L_{t_2}} = (C_{L\alpha})_{t,ss} \left(1 - \frac{i\omega y_t}{i\omega + \frac{z_t u}{c_{r_t}/2}} \right) \quad (30)$$

$$\tilde{C}_{L_e} = (C_{L\delta_e})_{ss} \left(1 - \frac{i\omega y_e}{i\omega + \frac{z_e u}{c_{r_e}/2}} \right) \quad (31)$$

Equations (25) and (26) can be solved simultaneously to obtain the frequency-response characteristics as

$$\begin{bmatrix} \tilde{\alpha} \\ \tilde{\delta}_e \end{bmatrix} = \begin{bmatrix} A'_{11} & A'_{12} \\ A'_{21} & A'_{22} \end{bmatrix}^{-1} \begin{bmatrix} -\frac{\rho u S_w}{2m} \tilde{C}_{L_e} \\ -\frac{\rho u^2 S_w l_t}{2I_Y} \tilde{C}_{L_e} \end{bmatrix} \quad (32)$$

where

$$A'_{11} = i\omega + \frac{\rho u S_w}{2m} (\tilde{C}_{L_w} + \tilde{C}_{L_{t_1}}) \quad (33)$$

$$A'_{12} = -1 + \frac{\rho S_w}{2m} \left[\left(\bar{x} + \frac{\bar{c}_w}{2} \right) \tilde{C}_{L_w} + \left(l_t + \frac{\bar{c}_t}{2} \right) \tilde{C}_{L_{t_2}} \right] \quad (34)$$

$$A'_{21} = \frac{\rho u^2 S_w \bar{c}_w}{2I_Y} \left[\frac{\bar{x}}{\bar{c}_w} \tilde{C}_{L_w} + \frac{l_t}{\bar{c}_w} \tilde{C}_{L_{t_1}} - (\tilde{C}_{m\alpha})_f \right] \quad (35)$$

$$A'_{22} = i\omega + \frac{\rho u S_w}{2I_Y} \left[\left(\bar{x} + \frac{\bar{c}_w}{2} \right) \bar{x} \tilde{C}_{L_w} + \left(l_t + \frac{\bar{c}_t}{2} \right) l_t \tilde{C}_{L_{t_2}} \right] \quad (36)$$

In the parameter-extraction mode, flight data in the form of time histories of α , q , and δ_e are converted to the frequency domain, and equations (25) and (26) are used in a parameter-extraction algorithm to extract parameters to best fit the frequency-domain data. However, some aspects of the equations are undesirable. First, the number of aerodynamic parameters in the equations is limited to $(C_{L\alpha})_{w,ss}$, $(C_{L\alpha})_{t,ss}$, $\left(\frac{\partial \epsilon}{\partial \alpha}\right)_{l,ss}$, $(C_{m\alpha})_f$, and $C_{L\delta_e}$. Some of these occur in combinations which multiply common states and, therefore, might be difficult to separate. Secondly, it would be preferable to extract aerodynamic parameters for the entire aircraft rather than those associated with aircraft components. These concerns led to the idea of examining the equations to determine whether some alterations could be made to obtain parameters in a more desirable form.

Unsteady aerodynamics are introduced into the equations of motion through the indicial lift and downwash equations. Results presented in reference 9 indicate that effects of unsteady aerodynamics on aircraft motion could be modeled reasonably accurately if indicial response in lift is omitted and unsteady effects are included only in the downwash behind the wing. It was decided to proceed under this condition and to check at a later point to determine whether the results justified making this simplification.

Indicial lift omitted.- Including unsteady aerodynamics in the downwash and omitting the indicial lift function simplify equations (27), (28), (30), and (31). Note that F_w' , G_w' , and H_w' , which appear in equation (29), also involve the indicial lift (see eqs. (12) and (15)) and must be modified. Equations (27), (28), (30), and (31) become

$$\tilde{C}_{L_w} = (C_{L\alpha})_{w,ss} \quad (37)$$

$$\left(\tilde{C}_{L_{t1}}\right)_s = (C_{L\alpha})_{t,ss} \left\{ \left[1 - \left(\frac{\partial \epsilon}{\partial \alpha}\right)_{l,t,ss} \right] + \left(\frac{\partial \epsilon}{\partial \alpha}\right)_{l,t,ss} \tilde{D} \right\} \quad (38)$$

$$\left(\tilde{C}_{L_{t2}}\right)_s = (C_{L\alpha})_{t,ss} \quad (39)$$

$$\left(\tilde{C}_{L_e}\right)_s = (C_{L\delta_e})_{ss} \quad (40)$$

where F_w' , G_w' , and H_w' , which appear in the \tilde{D} -term, are obtained by curve fitting equation (15) to equation (12) with $y = z = 0$. (See appendix A.) Equations (37) to (40) are then used in equations (25) and (26) to replace \tilde{C}_{L_w} , $\tilde{C}_{L_{t1}}$, $\tilde{C}_{L_{t2}}$, and \tilde{C}_{L_e} , respectively.

When unsteady effects are included only in the downwash, equations (25) and (26) with the use of equations (37) to (40) can be simplified and put into the forms

$$i\omega\tilde{\alpha} = \tilde{q} - \frac{\rho u S_w}{2m} \left\{ \left[(C_{L\alpha})_{w,ss} + (\tilde{C}_{L_{t1}})_s \right] \tilde{\alpha} + \left[\left(\bar{x} + \frac{\bar{c}_w}{2} \right) (C_{L\alpha})_{w,ss} + \left(l_t + \frac{\bar{c}_t}{2} \right) (C_{L\alpha})_{t,ss} \right] + (C_{L\delta_e})_{ss} \tilde{\delta}_e \right\} \quad (41)$$

and

$$i\omega\tilde{q} = - \frac{\rho u^2 S \bar{c}_w}{2I_Y} \left\{ \left[\frac{\bar{x}}{\bar{c}_w} (C_{L\alpha})_{w,ss} + \frac{l_t}{\bar{c}_w} (\tilde{C}_{L_{t1}})_s \right] \tilde{\alpha} + \left[\left(\bar{x} + \frac{\bar{c}_w}{2} \right) \frac{\bar{x}}{\bar{c}_w} (C_{L\alpha})_{w,ss} + \left(l_t + \frac{\bar{c}_t}{2} \right) \frac{l_t}{\bar{c}_w} (C_{L\alpha})_{t,ss} \right] \frac{\tilde{q}}{u} + \frac{l_t}{\bar{c}_w} (C_{L\delta_e})_{ss} \tilde{\delta}_e - (C_{m\alpha})_f \tilde{\alpha} \right\} \quad (42)$$

Some terms in equations (41) and (42) can be converted to more convenient forms. The first bracketed terms of equation (41) become, by using equation (38),

$$(C_{L\alpha})_{w,ss} + (\tilde{C}_{L_{t1}})_s = (C_{L\alpha})_{w,ss} + (C_{L\alpha})_{t,ss} \left[1 - \left(\frac{\partial \varepsilon}{\partial \alpha} \right)_{l_t,ss} \right] + (C_{L\alpha})_{t,ss} \left(\frac{\partial \varepsilon}{\partial \alpha} \right)_{l_t,ss} \tilde{D} \quad (43)$$

By assuming that the total lift of the airplane is contributed by the wing and tail

$$(C_{L\alpha})_{w,ss} + (C_{L\alpha})_{t,ss} \left[1 - \left(\frac{\partial \varepsilon}{\partial \alpha} \right)_{l_t,ss} \right] = (C_{L\alpha})_{ss} \quad (44)$$

and therefore

$$(C_{L\alpha})_{w,ss} + (\tilde{C}_{L_{t1}})_s = (C_{L\alpha})_{ss} + (C_{L\alpha})_{t,ss} \left(\frac{\partial \varepsilon}{\partial \alpha} \right)_{l_t,ss} \tilde{D} \quad (45)$$

The second bracketed term of equation (41) can be multiplied and divided by $\bar{c}_w/2$ to obtain

$$\left[\left(\frac{2\bar{x}}{\bar{c}_w} + 1 \right) (C_{L\alpha})_{w,ss} + \left(\frac{2\lambda_t}{\bar{c}_w} + \frac{\bar{c}_t}{\bar{c}_w} \right) (C_{L\alpha})_{t,ss} \right] \frac{\tilde{q}\bar{c}_w}{2u} = (C_{Lq})_{ss} \frac{\tilde{q}\bar{c}_w}{2u} \quad (46)$$

Some terms of equation (42) also can be combined. For example, the first bracketed term can be combined with $(C_{m\alpha})_f$ to obtain

$$-\left[\frac{\bar{x}}{\bar{c}_w} (C_{L\alpha})_{w,ss} + \frac{\lambda_t}{\bar{c}_w} (\tilde{C}_{Lt1})_s \right] + (C_{m\alpha})_f = (C_{m\alpha})_{ss} - \frac{\lambda_t}{\bar{c}_w} (C_{L\alpha})_{t,ss} \left(\frac{\partial \varepsilon}{\partial \alpha} \right)_{\lambda,ss} \tilde{D} \quad (47)$$

The second bracketed term of equation (42) can be shown to reduce to

$$-\left[\left(\bar{x} + \frac{\bar{c}_w}{2} \right) \frac{\bar{x}}{\bar{c}_w} (C_{L\alpha})_{w,ss} + \left(\lambda_t + \frac{\bar{c}_t}{2} \right) \frac{\lambda_t}{\bar{c}_w} (C_{L\alpha})_{t,ss} \right] \frac{\tilde{q}}{u} = C_{mq} \frac{\tilde{q}c}{2u} \quad (48)$$

Using equations (45) and (46) in equation (41), and equations (47) and (48) in equation (42), and the relationship $\frac{\lambda_t}{\bar{c}_w} (C_{L\delta_e})_{ss} = (C_{m\delta_e})_{ss}$ results in

$$i\omega\tilde{\alpha} = \tilde{q} - \frac{\rho u S_w}{2m} \left\{ \left[(C_{L\alpha})_{ss} + (C_{L\alpha})_{t,ss} \left(\frac{\partial \varepsilon}{\partial \alpha} \right)_{\lambda,ss} \tilde{D} \right] \tilde{\alpha} + \frac{\bar{c}_w}{2u} (C_{Lq})_{ss} \tilde{q} + (C_{L\delta_e})_{ss} \tilde{\delta}_e \right\} \quad (49)$$

and

$$i\omega\tilde{q} = \frac{\rho u^2 S_w \bar{c}_w}{2I_Y} \left\{ \left[(C_{m\alpha})_{ss} - \frac{\lambda}{\bar{c}_w} (C_{L\alpha})_{t,ss} \left(\frac{\partial \varepsilon}{\partial \alpha} \right)_{\lambda,ss} \tilde{D} \right] \tilde{\alpha} + \frac{\bar{c}_w}{2u} (C_{mq})_{ss} \tilde{q} + (C_{m\delta_e})_{ss} \tilde{\delta}_e \right\} \quad (50)$$

Equations (49) and (50) can be solved simultaneously to obtain the frequency-response characteristics as

$$\begin{bmatrix} \tilde{\alpha} \\ \tilde{q} \end{bmatrix} = \begin{bmatrix} A_{11} & A_{12} \\ A_{21} & A_{22} \end{bmatrix}^{-1} \begin{bmatrix} \frac{-\rho u S_w}{2m} (C_{L\delta_e})_{ss} \\ \frac{\rho u^2 S_w \bar{c}_w}{2I_Y} (C_{m\delta_e})_{ss} \end{bmatrix} \tilde{\delta}_e \quad (51)$$

where

$$A_{11} = i\omega + \frac{\rho u S_w}{2m} \left[(C_{L\alpha})_{ss} + (C_{L\alpha})_{t,ss} \left(\frac{\partial \epsilon}{\partial \alpha} \right)_{l_t,ss} \tilde{D} \right] \quad (52)$$

$$A_{12} = \rho \frac{S_w}{4m} \bar{c}_w (C_{Lq})_{ss} - 1 \quad (53)$$

$$A_{21} = \frac{-\rho u^2 S_w \bar{c}_w}{2I_Y} \left[(C_{m\alpha})_{ss} - \frac{l_t}{\bar{c}_w} (C_{L\alpha})_{t,ss} \left(\frac{\partial \epsilon}{\partial \alpha} \right)_{l_t,ss} \tilde{D} \right] \quad (54)$$

$$A_{22} = i\omega - \frac{\rho u S_w \bar{c}_w^2}{4I_Y} C_{mq} \quad (55)$$

and

$$\tilde{D} = \left\{ \left[\frac{2i\omega F_w}{u/c_{r_w}} e^{-\left(2\frac{l-c_{r_w}}{u}\right)i\omega} \right] \left[E_i \left(2\frac{l-c_{r_w}}{u} i\omega \right) \right] + \frac{i\omega G_w}{i\omega + \frac{H_w u}{c_{r_w}/2}} \right\} \quad (56)$$

As noted previously, the terms F_w , G_w , and H_w are determined by curve fitting equation (15) to equation (12) with $y = z = 0$. A numerical procedure for this purpose and results for a wide range of wing geometries are discussed in appendix A.

Equation (51) can be used for parameter extraction if the assumption that indicial lift effects can be ignored, as was assumed in the simplifications used to proceed from the complete equations (32) to (51), is valid.

Effects of Omitting Indicial Response From Equations of Motion

The two steps taken to examine the effects of neglecting indicial response are as follows:

(1) Determine whether the indicial lift has any effect on aircraft frequency-response characteristics.

(2) Determine whether indicial response influences the numerical value of extracted parameters.

The aircraft used in this part of the study is shown in figure 2 and has the mass and geometric characteristics of table I and the aerodynamic parameters of table II. This aircraft configuration was also used in flight tests discussed subsequently. The test aircraft had an all-movable tail for longitudinal control; therefore for this configuration $\tilde{C}_{L_e} = \tilde{C}_{L_{t_2}}$, and the problem of determining the indicial response for an elevator-type control did not have to be addressed.

The computed frequency-response characteristics for the aircraft configuration with and without the indicial lift function, but including unsteadiness in downwash, are shown in figure 3. Since the frequency-response characteristics are very similar for the two cases, it appears that the indicial lift function would have a minor influence on aircraft motion, which is in agreement with the results of reference 9. In order to perform step (2), the two sets of frequency-response characteristics were used in a parameter-extraction exercise, using the algorithm developed in appendix B. The results are given in table III and show that the two sets of extracted parameters are in close agreement except for C_{L_q} . Since C_{L_q} has only a minor effect on airplane motion, the agreement in the remaining parameters seemed to justify further using the simplified equation (51), which neglects lift indicial responses, for parameter-extraction purposes.

PARAMETER EXTRACTION

Equation (51), which includes unsteady aerodynamics only in the downwash, is used for parameter extraction. The procedure is to measure flight data as a function of time, convert the data to the frequency domain by using the discrete Fourier transform, and then use a parameter-extraction algorithm to estimate aerodynamic parameters to provide a fit to the data in some optimal manner. In the present study, the maximum likelihood algorithm outlined in appendix B was used for parameter extraction. In principle, it should be possible to extract the parameters $(C_{L_\alpha})_{ss}$, $(C_{L_q})_{ss}$, $(C_{L_{\delta_e}})_{ss}$, $(C_{m_\alpha})_{ss}$, $(C_{m_q})_{ss}$, and $(C_{m_{\delta_e}})_{ss}$, and the product $(C_{L_\alpha})_{t,ss} \left(\frac{\partial \epsilon}{\partial \alpha} \right)_{l,ss}$.

Computer-Generated Data

The frequency-response characteristics of figure 3, with unsteady effects only in the downwash, were used with two parameter-extraction algorithms: One included unsteady aerodynamics; the other neglected unsteady aerodynamics. In performing parameter estimation using the algorithm that included unsteady aerodynamics, initial values of the parameters were assumed. These values were offset from the values which had been used to generate the data. The extraction program which included unsteady aerodynamics was allowed to iterate on the six parameters and the product previously listed. Although the extraction program retrieved the values used in generating the data, several parameters were very highly correlated. Pair-wise correlations above 0.95 were obtained between

$(C_{m\alpha})_{ss}$, $(C_{mq})_{ss}$, and $(C_{L\alpha})_{t,ss} \left(\frac{\partial \epsilon}{\partial \alpha}\right)_{\lambda_{t,ss}}$. The probability of high correlations between these parameters had been anticipated because of the manner in

which the terms appear in equations (49) and (50). It had been hoped, however, that the frequency-dependent factor \tilde{D} would relieve the correlation problem. Since this did not occur, the extraction program was rerun with the product

$(C_{L\alpha})_{t,ss} \left(\frac{\partial \epsilon}{\partial \alpha}\right)_{\lambda_{t,ss}}$ fixed at its correct value. This time the program again

retrieved the correct aerodynamic parameters and all correlation coefficients were very low. It was therefore thought advisable to use this approach in subsequent parameter extractions to keep correlations reasonably low.

The next step in this study was to use the same computer-generated data (unsteadiness only in the downwash) and the parameter-extraction algorithm which neglected unsteady effects ($\tilde{D} = 0$). In this case it should be recognized that the unsteady aerodynamic effects would be absorbed in the extracted parameters. In particular the parameters approximated by

$$C'_{mq} = (C_{mq})_{ss} + C_{m\dot{\alpha}} \quad (57)$$

and

$$C'_{m\alpha} = (C_{m\alpha})_{ss} - \frac{\rho S_w \bar{c}_w C_{m\dot{\alpha}} C_{L\alpha}}{4m} \quad (58)$$

would be extracted (ref. 1). The second term on the right-hand side of each equation represents an approximation which accounts for frequency-dependent unsteady aerodynamics by use of constant factors.

The parameters extracted with the two algorithms are shown in table IV. The two sets of aerodynamic parameters produce almost identical frequency-response characteristics as shown in figure 4. As indicated previously, the difference between $(C_{mq})_{ss}$ and C'_{mq} is interpreted as $C_{m\dot{\alpha}}$. An approximate

expression for $C_{m\dot{\alpha}}$, which is valid for low frequencies and is generally referred to as the lag-in-downwash effect (ref. 10), is

$$C_{m\dot{\alpha}} = -2 \left(\frac{\lambda}{\bar{c}_w} \right)^2 \left(\frac{\partial \epsilon}{\partial \alpha} \right)_{l,ss} (C_{L\alpha})_{t,ss} \quad (59)$$

If the parameters of table II are substituted into equation (59), the estimated value for $C_{m\dot{\alpha}}$ is -7.33, which is very close to the difference between the extracted values of $C_{m\dot{q}}$ and $C_{m\dot{q}}'$ shown in table IV (i.e., a difference of -7.35). These results indicate that for this particular case unsteady aerodynamic effects as approximated by the parameter $C_{m\dot{\alpha}}$ can be estimated accurately by the lag-in-downwash effect.

The reduced value extracted for $C_{m\alpha}$ when unsteady aerodynamics are not in the extraction algorithm is also of the expected order of magnitude. In this case the extracted value should be (appendix A of ref. 1)

$$C_{m\alpha}' = (C_{m\alpha})_{ss} - \frac{\rho S_w \bar{c}_w C_{m\dot{\alpha}} C_{L\alpha}}{4m}$$

Using the geometric and mass characteristics of table I, the aerodynamic parameters used in generating the data, and the value of $C_{m\dot{\alpha}}$ based on the geometric parameters, $C_{m\alpha} = -1.30$, which is reasonably close to the value of -1.09 actually extracted.

Flight Data

The flight data used in this part of the study were obtained for a general-aviation light airplane having the configuration shown in figure 2. The geometric mass characteristics and flight conditions are given in table I, and the measured flight data are shown in figure 5 as time histories of various measured states. Because of the measured vertical acceleration used in the parameter estimation procedure, the transformed equations of motion were extended by the equation

$$\tilde{a}_z = \frac{u}{g} (i\omega\tilde{\alpha} - \tilde{q})$$

As noted previously, it is much more convenient, when using a mathematical model involving unsteady aerodynamics, to perform parameter extraction in the frequency domain. The data of figure 5 were converted to the frequency domain by use of the discrete Fourier transform, and are presented as part of figures 6 and 7. Parameter extraction was performed in two different modes:

(1) In the frequency domain, using the algorithm of appendix B with unsteady aerodynamic modeling included in the downwash.

(2) In the frequency domain, using the algorithm of appendix B with unsteady aerodynamics not modeled. In this case some of the extracted parameters, notably C_{m_q}' , reflect any unsteady effects.

First, an attempt was made to extract all six parameters of equation (51) plus the product $(C_{L\alpha})_{t,ss} \left(\frac{\partial \epsilon}{\partial \alpha} \right)_{l,ss}$. The problem of high correlation was encountered, as was the case with computer-generated data. In addition, however, some of the parameters were unrealistic in magnitude and/or sign. Parameter extraction then was performed with the product $(C_{L\alpha})_{t,ss} \left(\frac{\partial \epsilon}{\partial \alpha} \right)_{l,ss}$ held constant at an estimated value based on the wing and tail geometry. The parameters extracted in these two modes are given in table V, and the frequency-response characteristics obtained by using each set of parameters are shown in figures 6 and 7. Both sets of parameters, when used in their respective modeling equations, fit the flight-measured time histories equally well as judged by estimated residuals.

Since it is preferable to extract individual derivatives, performing identification with modeling of unsteady aerodynamics as proposed herein appears to be preferable to extracting combination derivatives. Application of the extraction algorithm in the two modes suggested, that is, with and without modeling unsteady aerodynamics, provides a convenient means of separating the steady-state and acceleration derivatives. An alternate method of obtaining estimates of individual steady-state and acceleration derivatives by special flight maneuvers is suggested in reference 11.

CONCLUDING REMARKS

A simple vortex system has been used to model unsteady aerodynamic effects into the longitudinal equations of motion of an aircraft. The equations of motion in the time domain had two problems relative to application for parameter extraction: (1) Only a limited number of aerodynamic parameters appeared in the equations; and (2) the solution of integro-differential equations led to lengthy computations. The second problem was circumvented by transforming to the frequency domain; however, the first problem (limited number of derivatives) remained. Subsequent calculations showed that unsteady aerodynamic effects were adequately accounted for when the unsteady effects were included only in the downwash. This condition permitted recasting the equations in the frequency domain so that the usual aerodynamic parameters were present in the equations.

A parameter-extraction algorithm based on this formulation for unsteady aerodynamics permitted extraction of the aerodynamic derivatives associated with steady-state motion. If unsteady aerodynamic effects are omitted from the extraction algorithm, the extracted parameters will include the effects of unsteady aerodynamics; that is, some of the extracted parameters are interpreted as combinations of steady-state and acceleration derivatives. Use of

the two parameter-extraction algorithms, one including and the other omitting unsteady aerodynamic effects, provides a means of estimating some acceleration derivatives. However, the acceleration derivatives obtained are constants that approximate the effects of frequency-dependent aerodynamic phenomena.

The primary objectives of this study, the inclusion of unsteady aerodynamics in the rigid-body motion of an aircraft and the development of a parameter-extraction program which includes unsteady aerodynamic effects, have been accomplished. Additional studies suggested are: (1) To determine whether repeated tests under the same flight conditions will yield parameters with smaller ensemble variance when the extraction algorithm accounts for unsteady aerodynamics; and (2) to determine whether the extracted parameters will show less variation for different control inputs than is observed when unsteady effects are not taken into account.

Langley Research Center
National Aeronautics and Space Administration
Hampton, VA 23665
October 11, 1979

APPENDIX A

CALCULATION OF F, G, AND H OF DOWNWASH EQUATION

The downwash equation for a unit step increase in angle of attack for a wing represented by the vortex system of figure 1 is given by

$$\Delta \epsilon_{\lambda} = \left(\frac{\partial \epsilon}{\partial \alpha} \right)_{\lambda, ss} \left(1 - ye^{-\frac{zut}{c_r/2}} \right) \left[\frac{f_1 + f_2(t) + f_3(t)}{f_1 + f_2(\infty) + f_3(\infty)} \right] \quad (A1)$$

The functions f_1 , $f_2(t)$, and $f_3(t)$ are defined by equations (7). As noted previously, it was found expedient to perform parameter identification in the frequency domain; however, this procedure led to another problem since equation (A1) could not be converted because of the apparent lack of Laplace transforms for some of the terms involved in equation (A1). It had been found, during the study of reference 4, that for several representative wings, numerical results from equation (A1) could be approximated very closely by an expression of the form

$$\Delta \epsilon_{\lambda} = \left(\frac{\partial \epsilon}{\partial \alpha} \right)_{\lambda, ss} \left(1 - \frac{F}{\frac{l}{c_r} - 1 - \frac{ut}{2c_r}} - Ge^{-\frac{Hut}{c_r/2}} \right) \quad (A2)$$

where F, G, and H are functions of wing geometry and distance behind the wing root quarter-chord point. Laplace transforms of the various terms of equation (A2) are readily available.

In the present study, the constants F, G, and H were computed for a wide range of wing geometric characteristics by generating time histories of $\Delta \epsilon_{\lambda}$ using equation (A1), and then using a nonlinear least-squares procedure to determine values of F, G, and H which caused equation (A2) to provide the best fit to the time histories using the least-squares method. The procedure was to compute $\Delta \epsilon_{\lambda}$ at 40 equally spaced intervals, starting at a low value of ut/c_r and extending to a value for which $\Delta \epsilon_{\lambda}$ was essentially constant (fig. 8). These values were used as measured data y_m . An initial guess was then made of a parameter vector θ containing as its elements the constants F, G, and H. These initial guesses were used in equation (A2) to estimate $\Delta \epsilon_{\lambda}$, which was treated as computed data y_c . Sensitivity coefficients were computed analytically from equation (A2) and are

APPENDIX A

$$\left. \begin{aligned}
 A_1 &= \frac{\partial y_c}{\partial F} = - \frac{1}{\frac{l}{c_r} - 1 - \frac{ut}{2c_r}} \\
 A_2 &= \frac{\partial y_c}{\partial G} = -e^{-\frac{Hut}{c_r/2}} \\
 A_3 &= \frac{\partial y_c}{\partial H} = G \frac{ut}{c_r/2} e^{-\frac{Hut}{c_r/2}}
 \end{aligned} \right\} \quad (A3)$$

The sensitivity coefficients formed a row matrix A. An iteration procedure was then used to converge on the values of F, G, and H to best fit the measured data y_m by using parameter updates computed from

$$\Delta\theta = \left(\sum_i A_i^T A_i \right)^{-1} \left\{ \sum_i A_i^T [y_m - y_c(\theta_0)]_i \right\} \quad (A4)$$

The updated parameter vector is

$$\theta = \theta_0 + \Delta\theta \quad (A5)$$

where θ_0 is the initial parameter vector. Iterations are continued until the parameter update is judged to be negligible or until the fit to the data meets some convergence criteria. This procedure was used to calculate the constants for a wide range of values of wing geometry (A, λ , and Λ) and distance behind the wing root quarter-chord point. The results are given in figure 9.

APPENDIX B

MAXIMUM LIKELIHOOD IDENTIFICATION ALGORITHM

The parameter-estimation algorithm used in this study is the maximum likelihood technique in the frequency domain (ref. 12). This method provides consistent estimates and has the asymptotic properties of unbiased and minimum variance estimates. The method which is based on maximization of the likelihood function yields the parameter-estimation algorithm and the covariance matrix for the parameters. In a separate step maximization of the likelihood function yields the covariance matrix for the measurement noise based on the current nominal solution.

Let θ be the vector of unknown parameters. The maximum likelihood estimation is based on maximizing the conditional probability density of $\tilde{z}(n)$ given θ or maximizing the log likelihood function L given as

$$\begin{aligned} L(\theta) &= N \operatorname{Re} \sum_n [\tilde{z}(n) - \tilde{x}(n, \theta_0)]^* R^{-1} [\tilde{z}(n) - \tilde{x}(n, \theta_0)] \\ &\quad - \frac{N}{2} \log |R| - \text{Constant} \\ &= N \operatorname{Re} \sum_n \tilde{v}(n)^* R^{-1} \tilde{v}(n) - \frac{N}{2} \log |R| - \text{Constant} \end{aligned} \quad (\text{B1})$$

where $\tilde{z}(n)$ is the vector of measured variables and $\tilde{x}(n, \theta_0)$ is the vector of computed output variables.

To estimate R , the likelihood function is maximized with respect to the elements in R and thereby yields

$$\hat{R} = \operatorname{diag} \left[\frac{1}{N} \sum_n \tilde{v}(n) \tilde{v}^*(n) \right] \quad (\text{B2})$$

For the estimates of the remaining parameters, the minimum of $L(\theta)$ is found by using the modified Newton-Raphson method. The estimates are given by

$$\theta = \theta_0 + \Delta\theta \quad (\text{B3})$$

where θ_0 is the current estimate of parameter vector, $\Delta\theta$ updates in the estimates of parameters, and $\Delta\theta = -M^{-1}g$ where M and g are, respectively, second and first gradients of the log-likelihood function.

For fixed $R = \hat{R}$

$$g_k = \frac{\partial L(\theta)}{\partial \theta_k} = -\text{Re} \sum_n \frac{\partial \tilde{v}^*}{\partial \theta_k} \hat{R}^{-1} \tilde{v} \quad (\text{B4})$$

and

$$M_{k\ell} = \frac{\partial^2 L(\theta)}{\partial \theta_k \partial \theta_\ell} \approx -\text{Re} \sum_n \frac{\partial \tilde{v}^*}{\partial \theta_k} \hat{R}^{-1} \frac{\partial \tilde{v}}{\partial \theta_\ell} \quad (\text{B5})$$

That is,

$$\Delta \theta = \left(\text{Re} \sum_n \frac{\partial \tilde{v}^*}{\partial \theta} \hat{R}^{-1} \frac{\partial \tilde{v}}{\partial \theta} \right)^{-1} \left(\text{Re} \sum_n \frac{\partial \tilde{v}^*}{\partial \theta} \hat{R}^{-1} \tilde{v} \right) \quad (\text{B6})$$

The effect of maximizing the likelihood function is the same as minimizing cost function (fit error)

$$J = \det \left[\frac{1}{N} \text{diag} \sum_n \tilde{v}(n) \tilde{v}^*(n) \right]$$

Generally, in a convergent-estimation process, the fit improved with iteration as evidenced by a reduction in the cost function. Once the cost function settled so that change in two successive iterations, as defined by $(J_k - J_{k-1})/J_k$, was less than 0.01, the parameters which maximize the likelihood function or minimize the fit error were considered identified.

The maximum likelihood identification algorithm proceeds in the following manner:

- (1) Choose a nominal value for parameter vector θ_0 and calculate $J(\theta_0)$.
- (2) From the equations of motion obtain $\tilde{x}(\theta_0, n)$ and the sensitivity function $\frac{\partial \tilde{v}(\theta_0, n)}{\partial \theta}$ using finite-difference methods.
- (3) Compare the transformed flight data with the chosen nominal.
- (4) Calculate an update of θ from the maximum likelihood estimate.
- (5) Calculate $J(\theta)$ and compare with $J(\theta_0)$.
- (6) Update the nominal parameter vector and continue until convergence.

REFERENCES

1. Klein, Vladislav: Determination of Stability and Control Parameters of a Light Airplane From Flight Data Using Two Estimation Methods. NASA TP-1306, 1979.
2. Morino, Luigi: A General Theory of Unsteady Compressible Potential Aerodynamics. NASA CR-2464, 1974.
3. Piszkin, S. T.; and Levinsky, E. S.: Nonlinear Lifting Line Theory for Predicting Stalling Instabilities on Wings of Moderate Aspect Ratio. Rep. No. CASD-NSC-76-001, U.S. Navy, June 15, 1976. (Available from DDC as AD A027 645.)
4. Edwards, John William: Unsteady Aerodynamic Modeling and Active Aeroelastic Control. SUDAAR 504 (NASA Grant NGL-05-020-007), Stanford Univ., Feb. 1977. (Available as NASA CR-148019.)
5. Wells, William R.; and Queijo, M. J.: Simplified Unsteady Aerodynamic Concepts, With Application to Parameter Estimation. Atmospheric Flight Mechanics Conference, Aug. 1977, pp. 39-45. (Available as AIAA Paper 77-1124.)
6. Queijo, M. J.; Wells, William R.; and Keskar, Dinesh A.: Approximate Indicial Lift Function for Tapered, Swept Wings in Incompressible Flow. NASA TP-1241, 1978.
7. Jones, Robert T.: Operational Treatment of the Nonuniform-Lift Theory in Airplane Dynamics. NACA TN 667, 1938.
8. Karamcheti, Krishnamurty: Principles of Ideal-Fluid Aerodynamics. John Wiley & Sons, Inc., c.1966.
9. Statler, I. C.: Dynamic Stability at High Speeds From Unsteady Flow Theory. J. Aero. Sci., vol. 17, no. 4, Apr. 1950, pp. 232-242, 255.
10. Etkin, Bernard: Dynamics of Atmospheric Flight. John Wiley & Sons, Inc., c.1972.
11. Maine, Richard E.; and Iliff, Kenneth W.: Maximum Likelihood Estimation of Translational Acceleration Derivatives From Flight Data. AIAA Paper 78-1342, Aug. 1978.
12. Klein, V.: Aircraft Parameter Estimation in Frequency Domain. A Collection of Technical Papers - AIAA Atmospheric Flight Mechanics Conference, Aug. 1978, pp. 140-147. (Available as AIAA Paper 78-1344.)

TABLE I.- GEOMETRIC AND MASS CHARACTERISTICS OF AIRCRAFT USED TO
 STUDY VARIOUS EFFECTS OF UNSTEADY AERODYNAMICS AND USED TO
 GENERATE FREQUENCY-RESPONSE CURVES OF FIGURE 3

Wing:	
Aspect ratio	7.35
Taper ratio	1.00
Sweep angle, deg	0
Root chord, m	1.34
Area, m ²	13.56
Horizontal tail:	
Aspect ratio	4.21
Taper ratio	1.00
Sweep angle, deg	0
Root chord, m	0.77
Area, m ²	2.51
Weight, N	9230
I _y , kg-m ²	2135
\bar{x} , m	0.116
\bar{c}_w , m	1.34
l _t , m	4.49
l, m	4.38
u, m/sec	47.5
ρ, kg/m ³	1.076

TABLE II.- AERODYNAMIC CHARACTERISTICS OF AIRCRAFT USED TO STUDY
 VARIOUS EFFECTS OF UNSTEADY AERODYNAMICS AND USED TO GENERATE
 FREQUENCY-RESPONSE CURVES OF FIGURE 3

	Indicial lift and unsteady downwash		Unsteady downwash only	
	Wing	Horizontal tail	Wing	Horizontal tail
Y, m	0.432	0.380	0	0
z, m	0.322	0.371	0	0
F'	1.3581		-----	
G'	0.5103		-----	
H'	0.0648		-----	
F	-----		1.4636	
G	-----		0.530	
H	-----		0.0648	
$(C_{L\alpha})_{w,ss}$	4.795		4.795	
$(C_{L\alpha})_{t,ss}$	0.74		0.74	
$(C_{L\delta_e})_{ss}$	0.74		0.74	
$(C_{m\alpha})_{f,ss}$	0.30		0.30	
$\left(\frac{\partial \epsilon}{\partial \alpha}\right)_{\lambda,ss}$	0.44		0.44	

TABLE III.- EFFECT OF INDICIAL LIFT FUNCTION ON EXTRACTED PARAMETERS,
USING COMPUTER-GENERATED DATA^a

Parameter	Extracted parameter value (b)	
	Data generated with unsteady downwash and indicial lift function	Data generated with unsteady downwash but without indicial lift function
$C_{L\alpha}$	5.38 (0.030)	5.21 (0)
$C_{L\delta_e}$.67 (.019)	.74 (0)
C_{Lq}	4.90 (.600)	11.02 (0)
$C_{m\alpha}$	-1.40 (.006)	-1.50 (0)
C_{mq}	-16.62 (.250)	-18.58 (0)
$C_{m\delta_e}$	-2.30 (.014)	-2.48 (0)
$(C_{L\alpha})_{t,ss} \left(\frac{\partial \epsilon}{\partial \alpha} \right)_l$	^c .33	^c .33

^aParameter-extraction algorithm included unsteady aerodynamics in downwash but had no indicial lift function.

^bValues in parentheses are variances (Cramér-Rao lower bound).

^cValue held constant during extraction.

TABLE IV.- RESULTS FROM PARAMETER EXTRACTION, USING COMPUTER-GENERATED
DATA WITH UNSTEADINESS ONLY IN DOWNWASH

Value used in generating data	Extracted value (a)	
	Extracted algorithm included unsteady effects in downwash	Extracted algorithm neglected all unsteady effects
$(C_{L\alpha})_{ss} = 5.21$	$(C_{L\alpha})_{ss} = 5.21 (0)$	$(C_{L\alpha})_{ss} = 4.92 (0.004)$
$(C_{Lq})_{ss} = 11.02$	$(C_{Lq})_{ss} = 11.02 (0)$	$(C_{Lq})_{ss} = 19.11 (0.700)$
$(C_{L\delta_e})_{ss} = 0.74$	$(C_{L\delta_e})_{ss} = 0.74 (0)$	$(C_{L\delta_e})_{ss} = 0.82 (0.002)$
$(C_{m\alpha})_{ss} = -1.50$	$(C_{m\alpha})_{ss} = -1.50 (0)$	$C'_{m\alpha} = -1.09 (0.010)$
$(C_{mq})_{ss} = -18.58$	$(C_{mq})_{ss} = -18.58 (0)$	$C'_{mq} = -25.93 (0.370)$
$(C_{m\delta_e})_{ss} = -2.48$	$(C_{m\delta_e})_{ss} = -2.48 (0)$	$C'_{m\delta_e} = -2.32 (0.020)$
$(C_{L\alpha})_{t,ss} \left(\frac{\partial \epsilon}{\partial \alpha}\right)_{l,ss} = 0.33$	$(C_{L\alpha})_{t,ss} \left(\frac{\partial \epsilon}{\partial \alpha}\right)_{l,ss} = {}^b 0.33$	$(C_{L\alpha})_{t,ss} \left(\frac{\partial \epsilon}{\partial \alpha}\right)_{l,ss} = {}^b 0.33$

^aValues in parentheses are variances (Cramér-Rao lower bound).

^bValue held constant during extraction.

TABLE V.- AERODYNAMIC PARAMETERS EXTRACTED FROM
FLIGHT DATA OF FIGURE 5

Extraction algorithm included unsteady effects in downwash (a)	Extraction algorithm neglected all unsteady effects (a)
$(C_{L\alpha})_{ss} = 5.12 (0.05)$	$(C_{L\alpha})_{ss} = 4.91 (0.03)$
$(C_{Lq})_{ss} = 4.69 (0.17)$	$(C_{Lq})_{ss} = 6.33 (0.33)$
$(C_{L\delta_e})_{ss} = 1.42 (0.07)$	$(C_{L\delta_e})_{ss} = 1.14 (0.05)$
$(C_{m\alpha})_{ss} = -1.34 (0.01)$	$C_{m\alpha}' = -0.99 (0.01)$
$(C_{mq})_{ss} = -15.37 (0.01)$	$C_{mq}' = -20.77 (0.58)$
$(C_{m\delta_e})_{ss} = -3.25 (0.05)$	$C_{m\delta_e}' = -2.95 (0.01)$
$(C_{L\alpha})_{t,ss} \left(\frac{\partial \epsilon}{\partial \alpha}\right)_{l,ss} = {}^b 0.33$	$(C_{L\alpha})_{t,ss} \left(\frac{\partial \epsilon}{\partial \alpha}\right)_{l,ss} = {}^b 0.33$

^aValues in parentheses are variances (Cramér-Rao lower bound).
^bValue held constant during extraction.

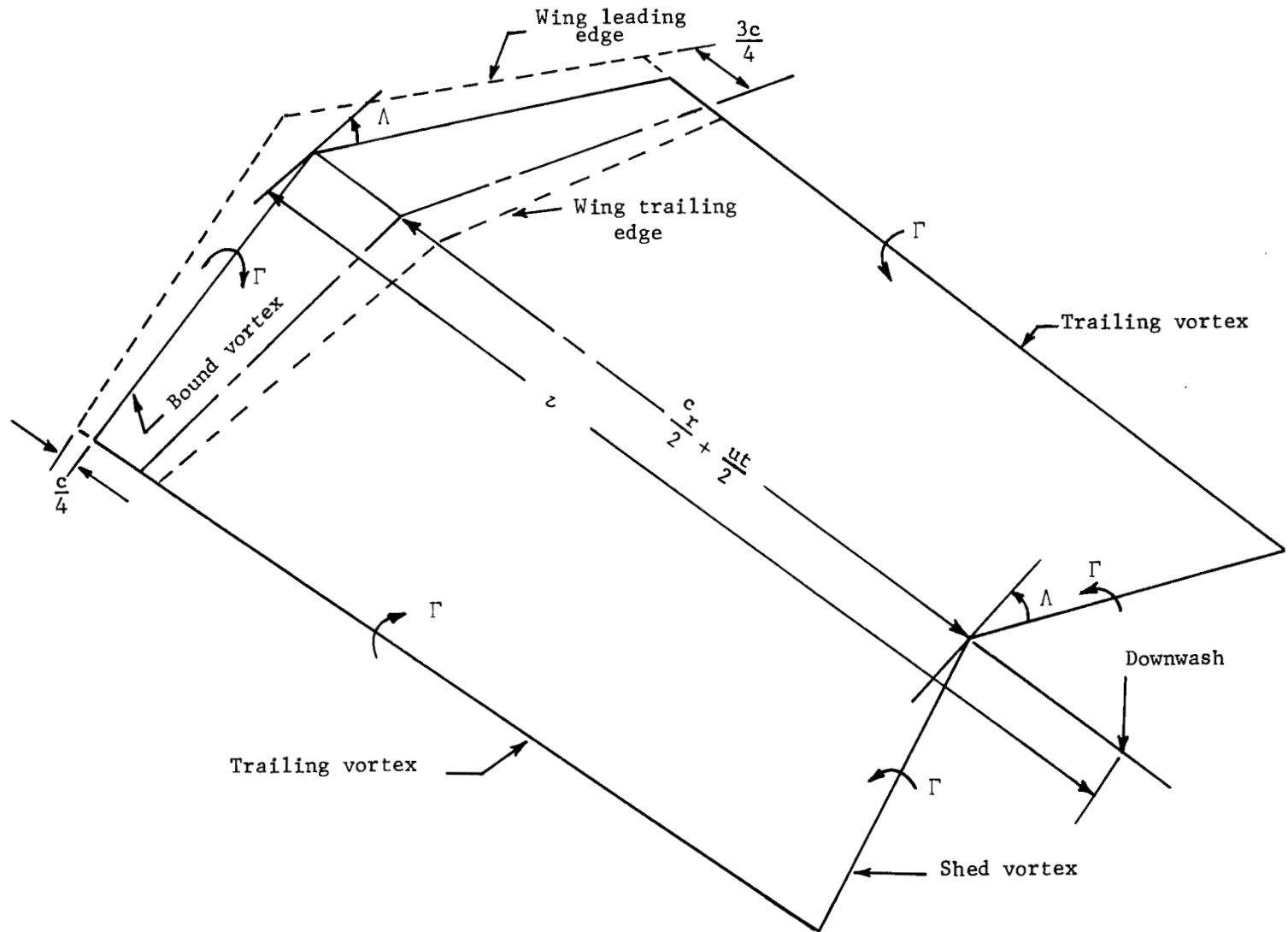


Figure 1.- Vortex system used for computing downwash.

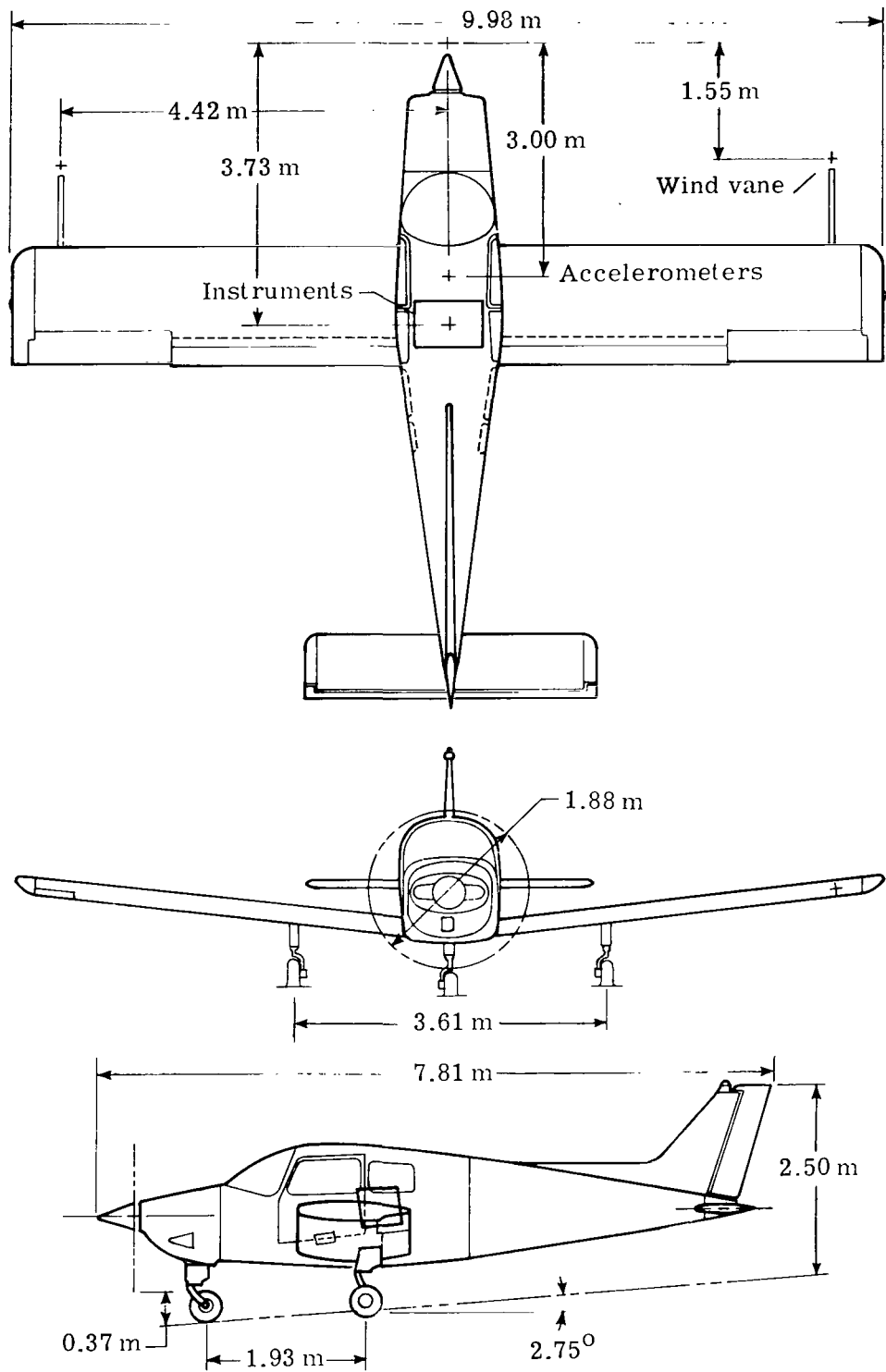
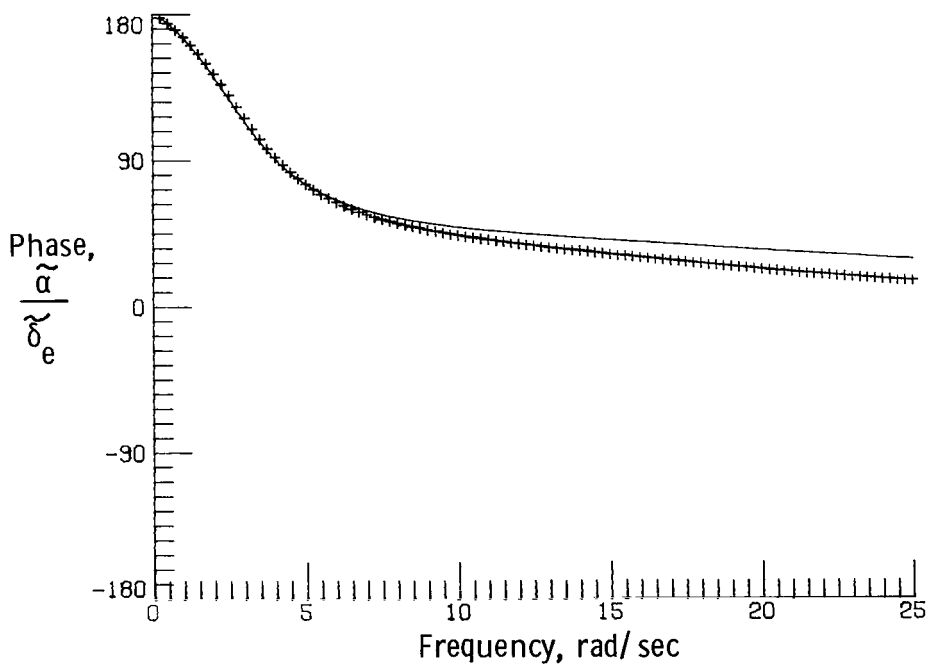
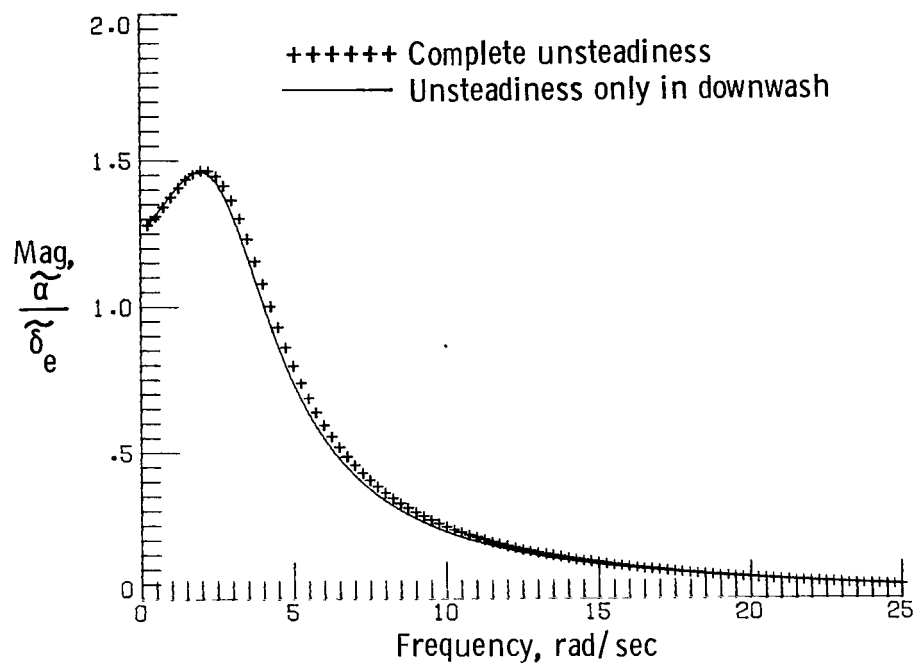
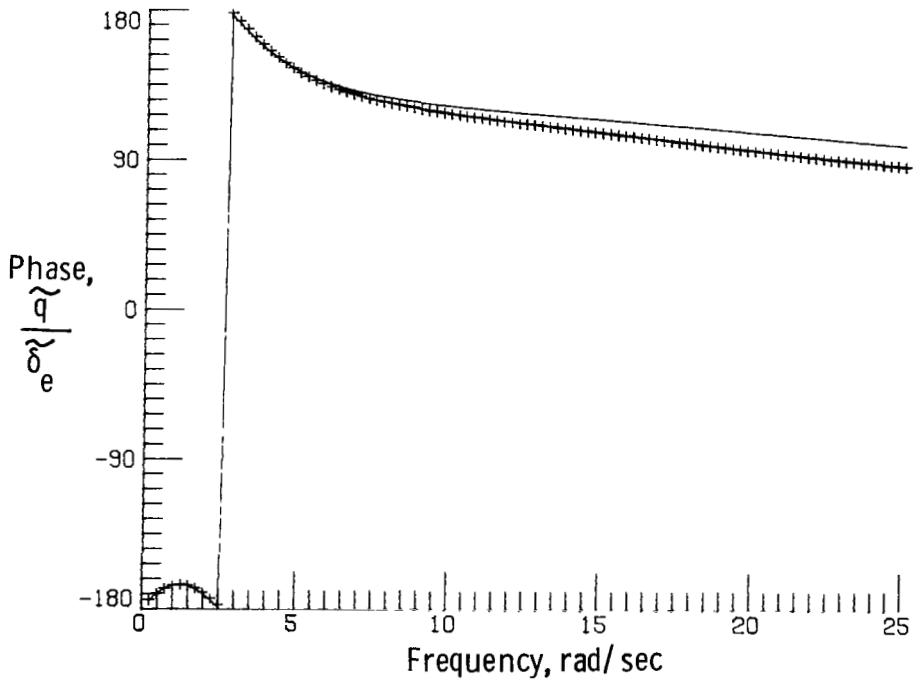
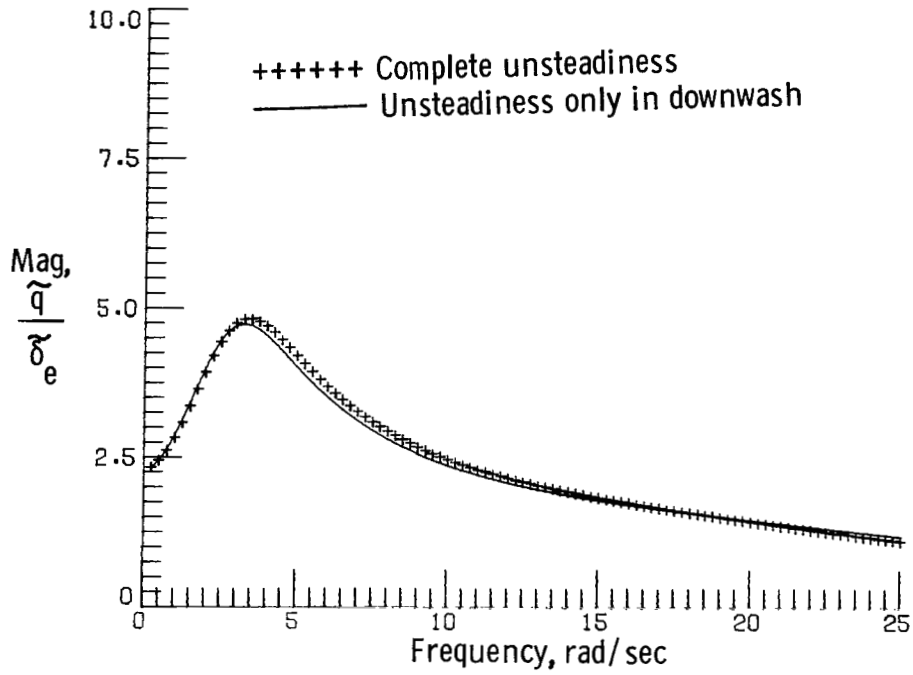


Figure 2.- Three-view drawing of test aircraft.



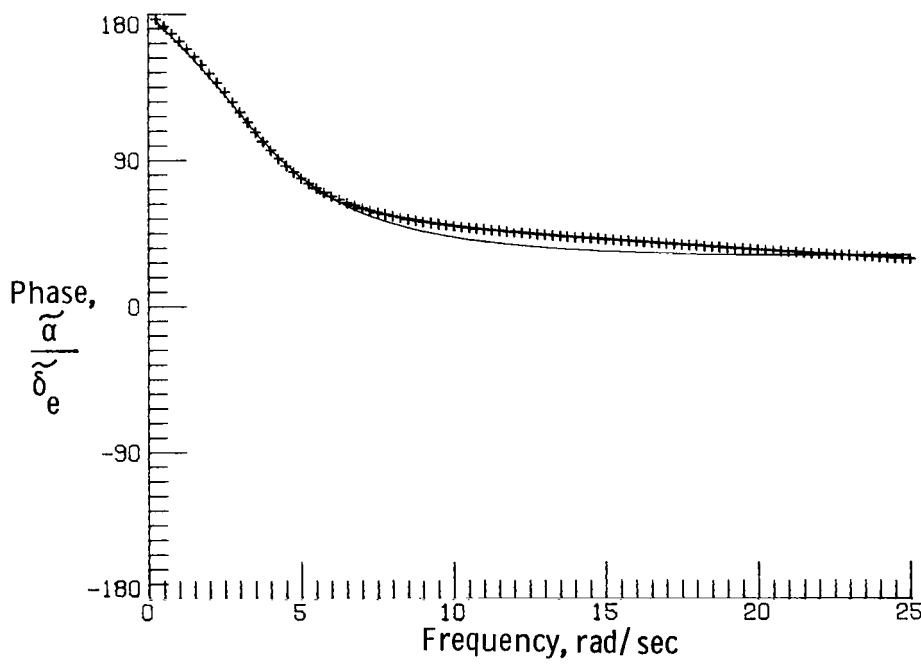
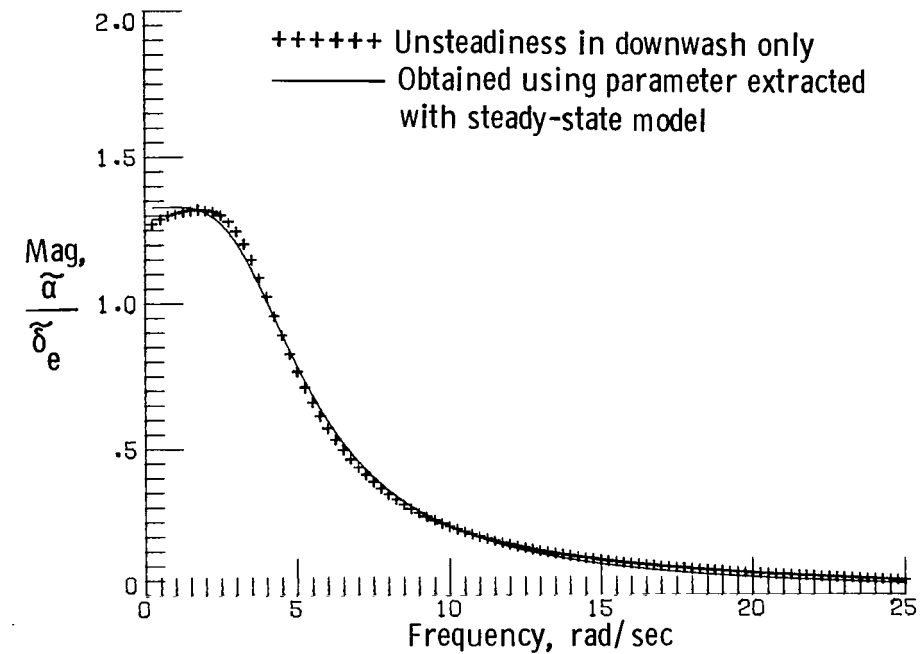
(a) Angle-of-attack response.

Figure 3.- Effects of unsteady aerodynamics on longitudinal response. Computer-generated data.



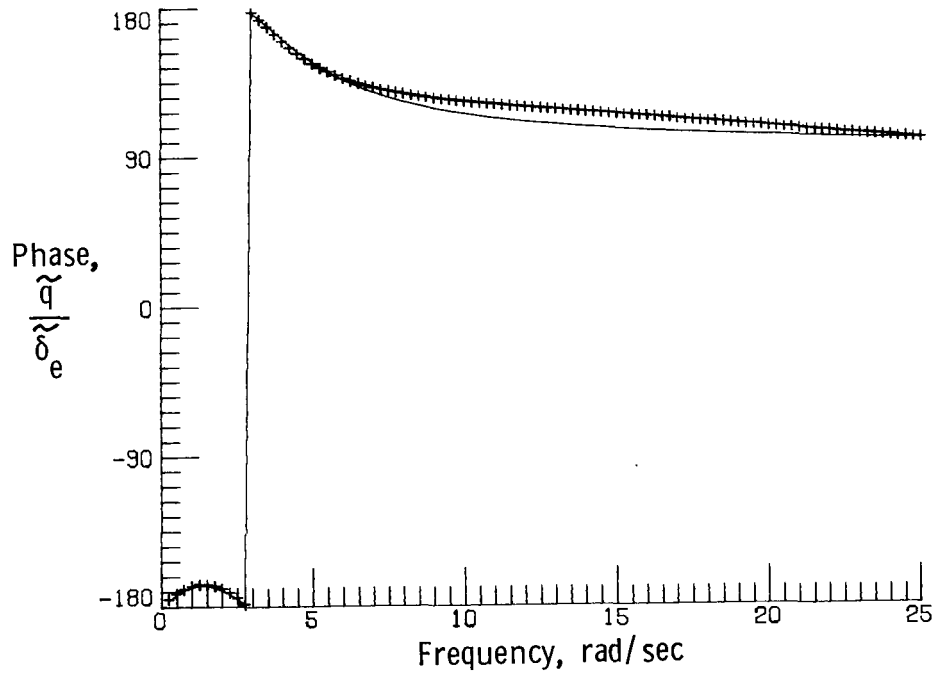
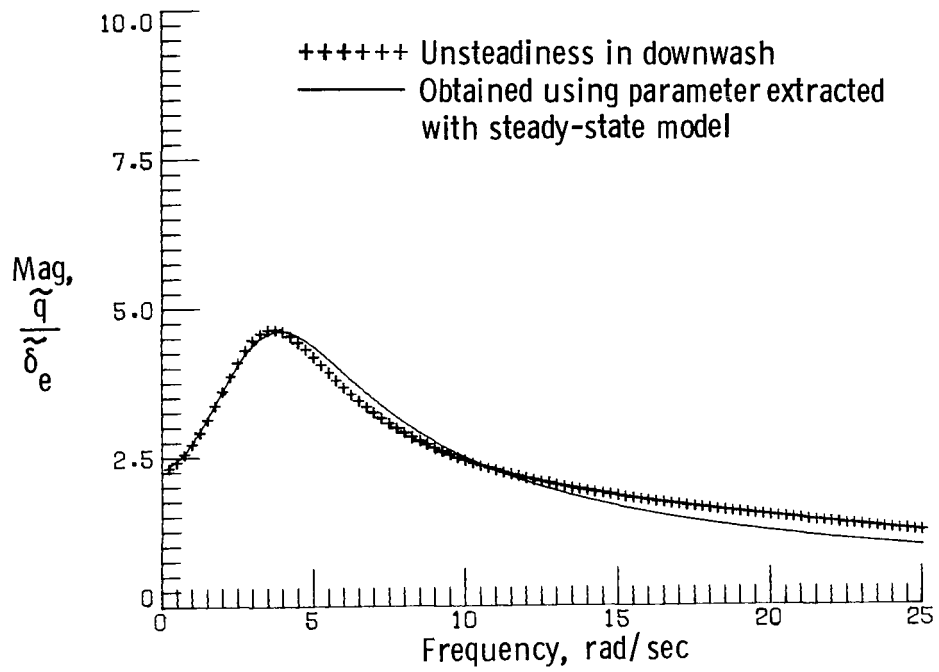
(b) Pitch-rate response.

Figure 3.- Concluded.



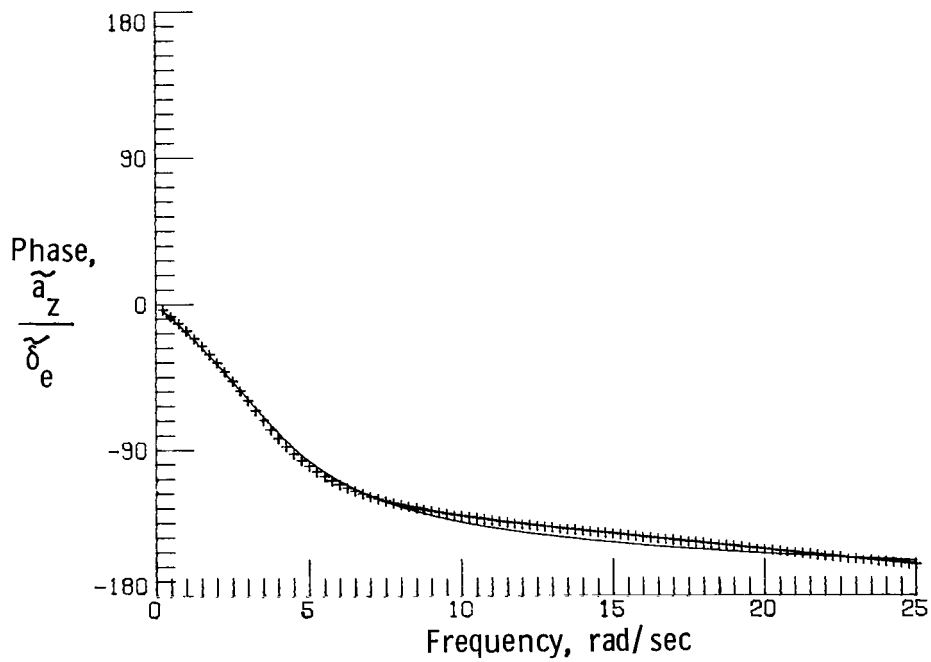
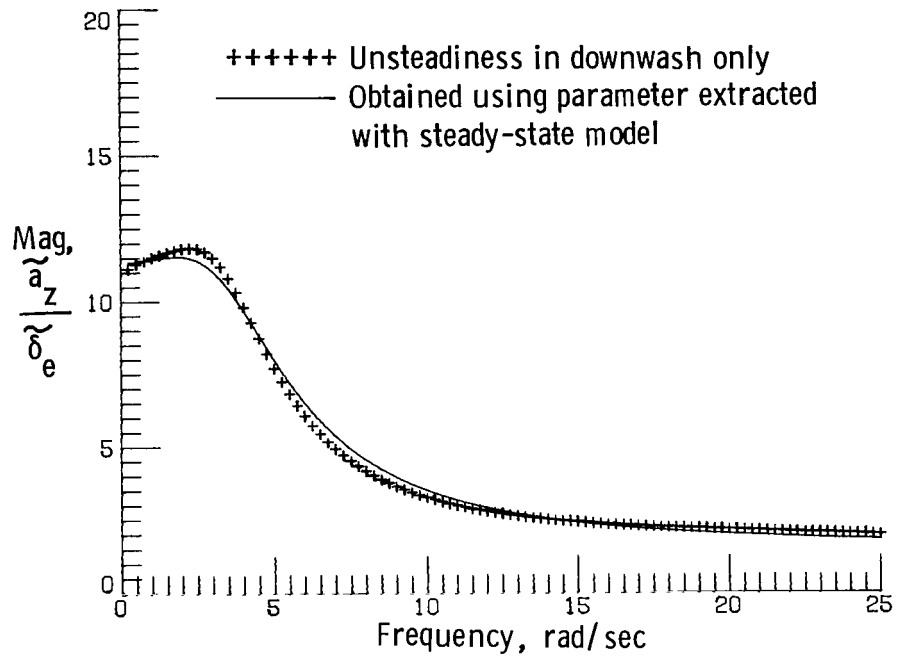
(a) Angle-of-attack response.

Figure 4.- Computer-generated data with unsteadiness only in downwash and data computed using parameters extracted by maximum likelihood method with unsteady effects neglected (steady-state model).



(b) Pitch-rate response.

Figure 4.- Continued.



(c) Normal-acceleration response.

Figure 4.- Concluded.

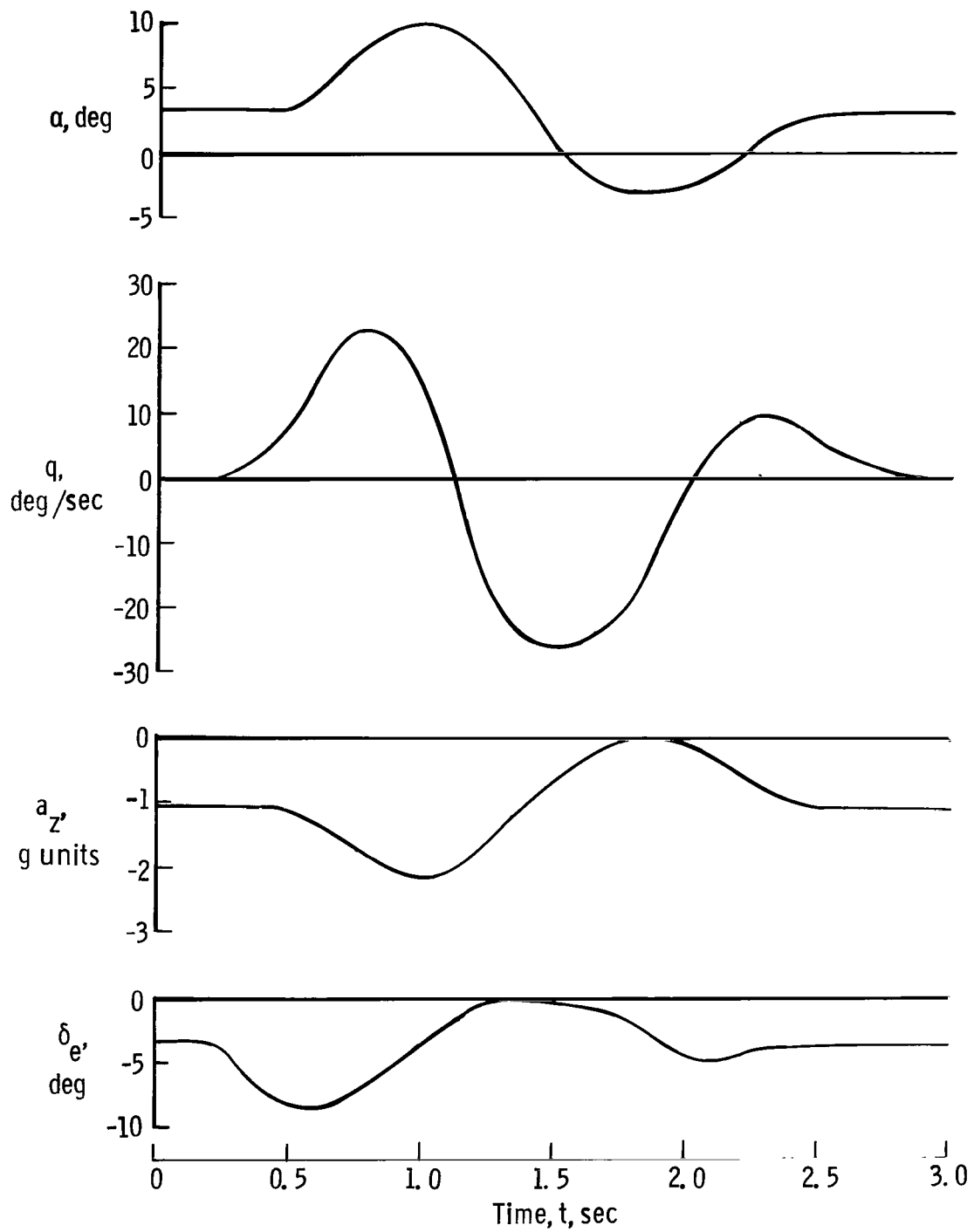
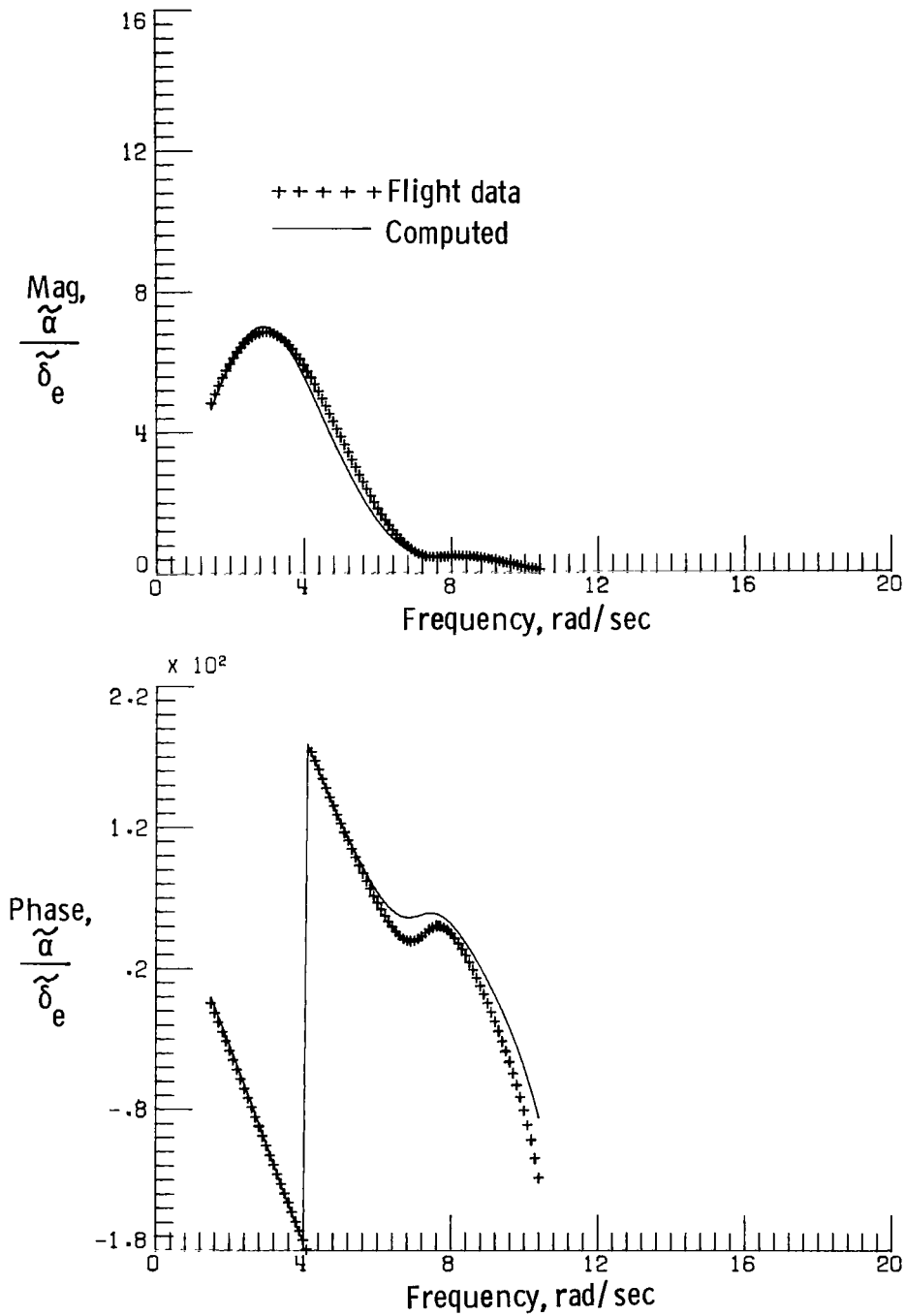
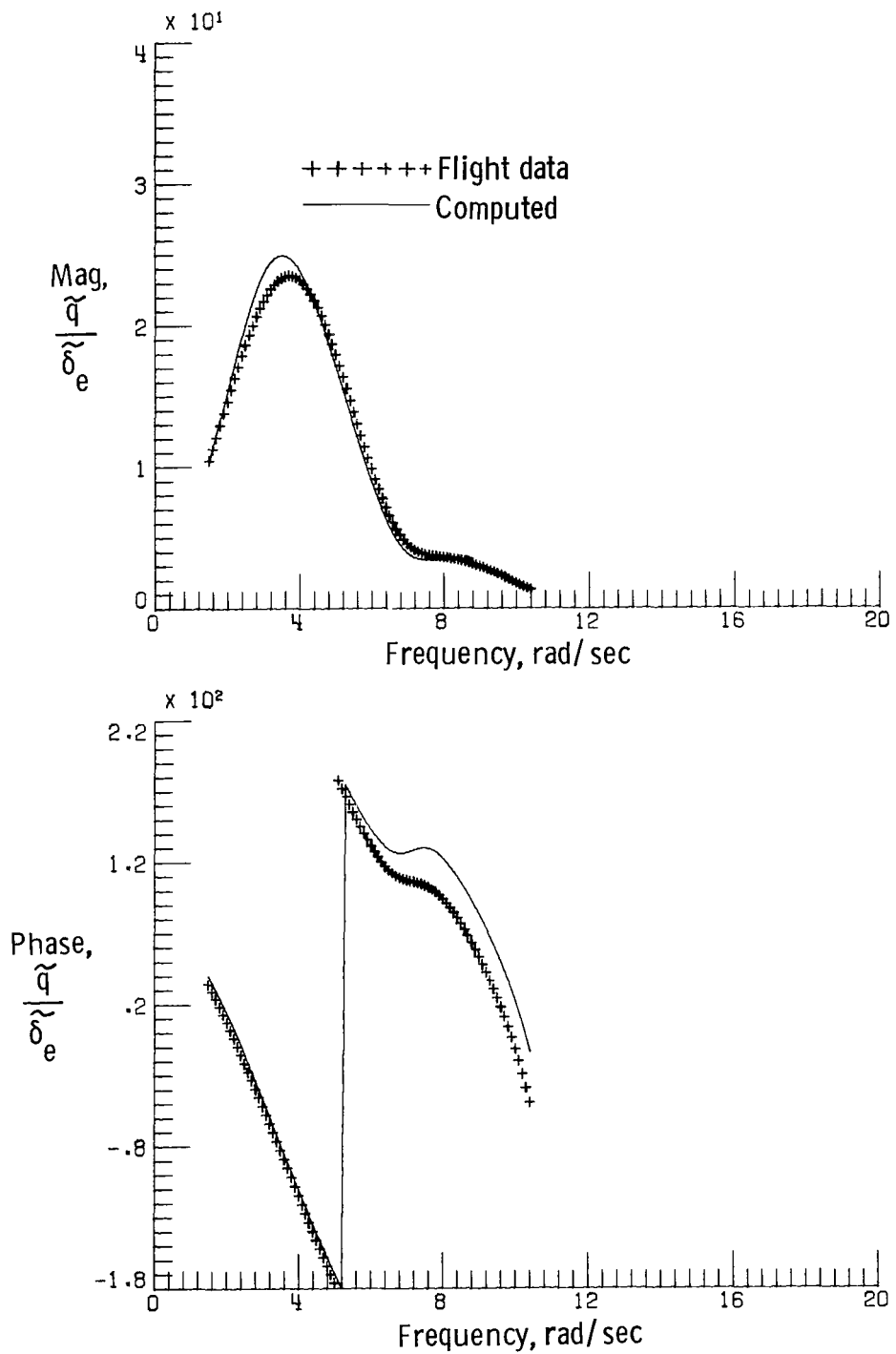


Figure 5.- Time histories of data measured from aircraft of figure 2.



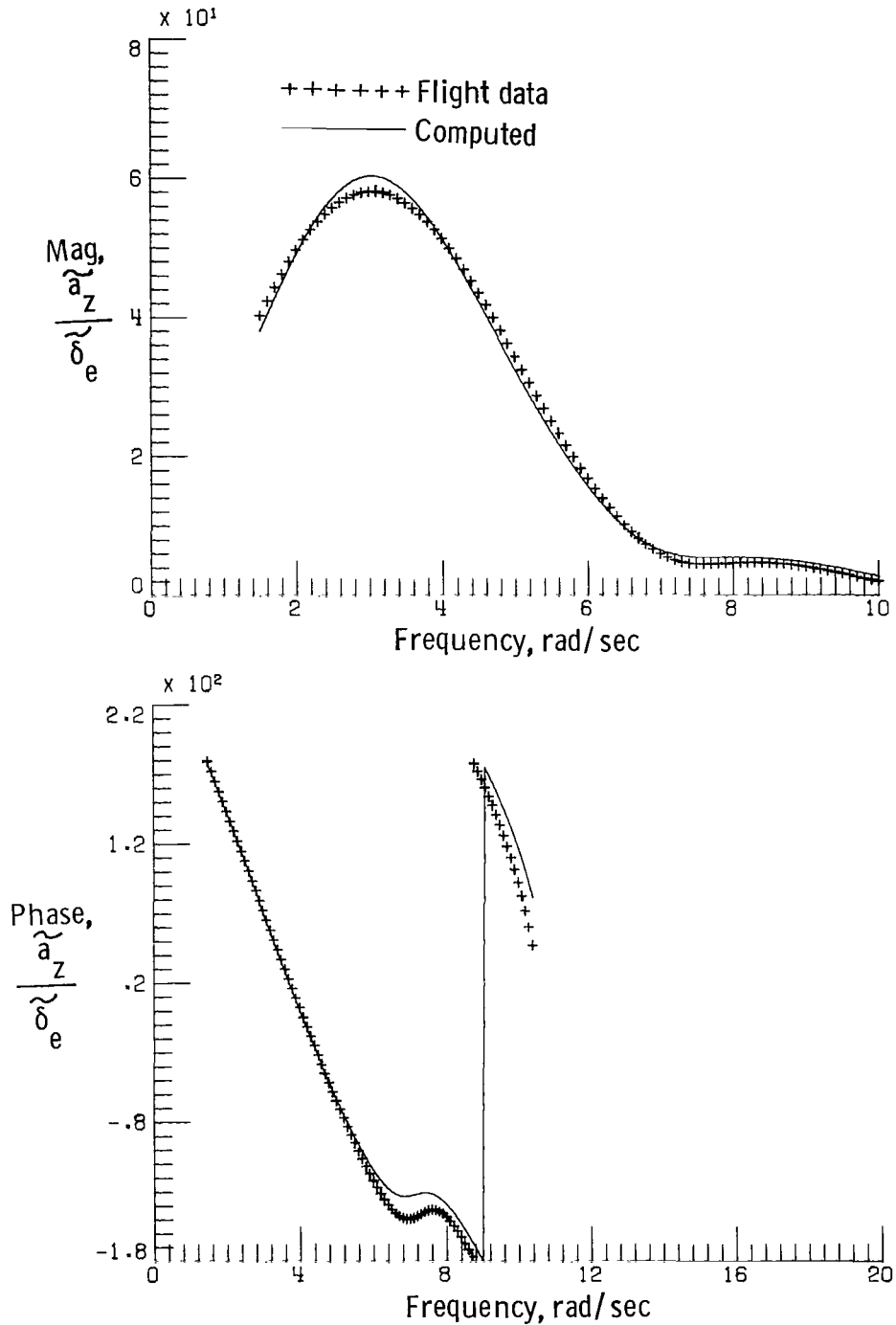
(a) Angle-of-attack response.

Figure 6.- Flight test data in frequency domain and data computed using extracted parameters when extraction algorithm included unsteady aerodynamics in downwash.



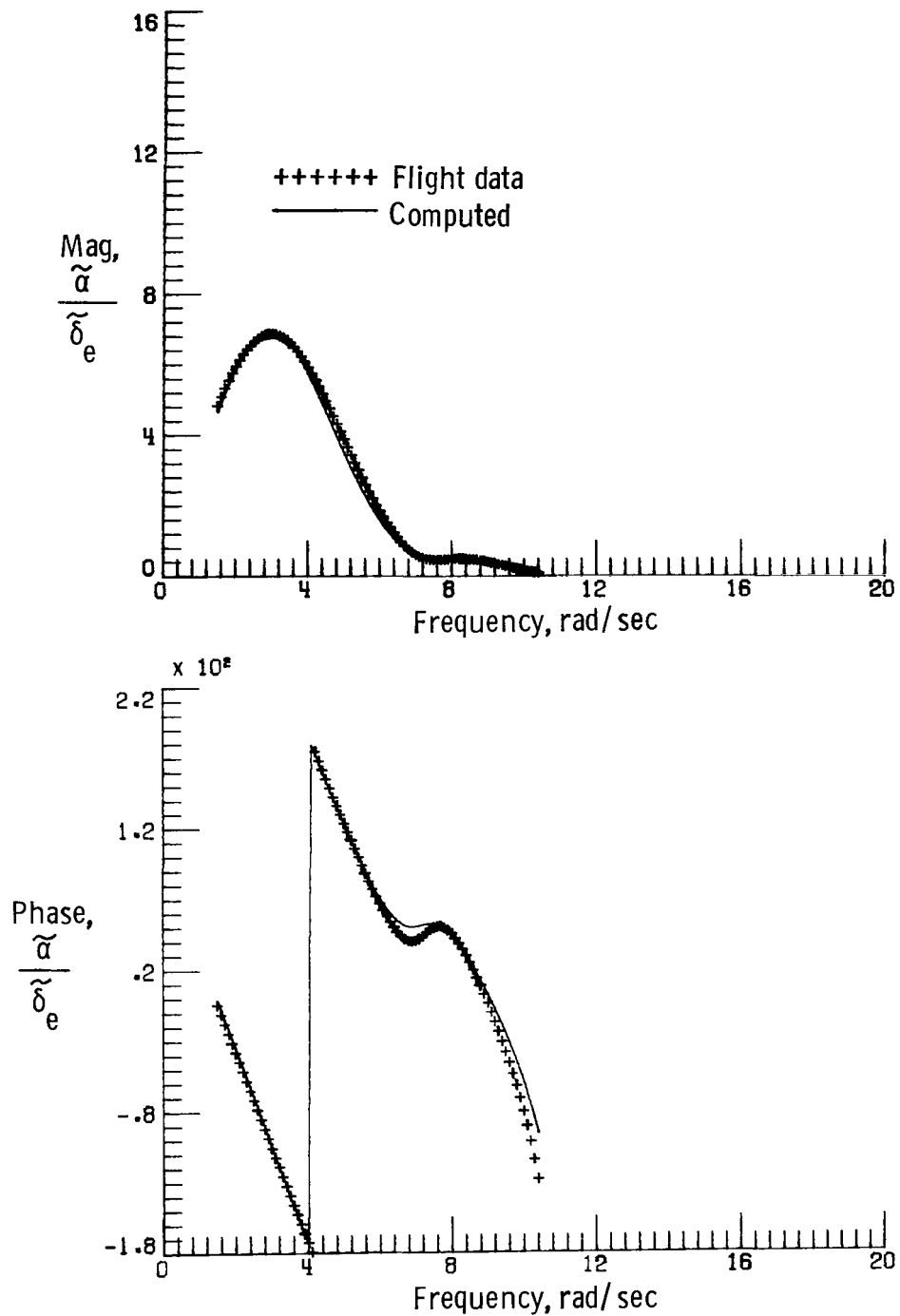
(b) Pitch-rate response.

Figure 6.- Continued.



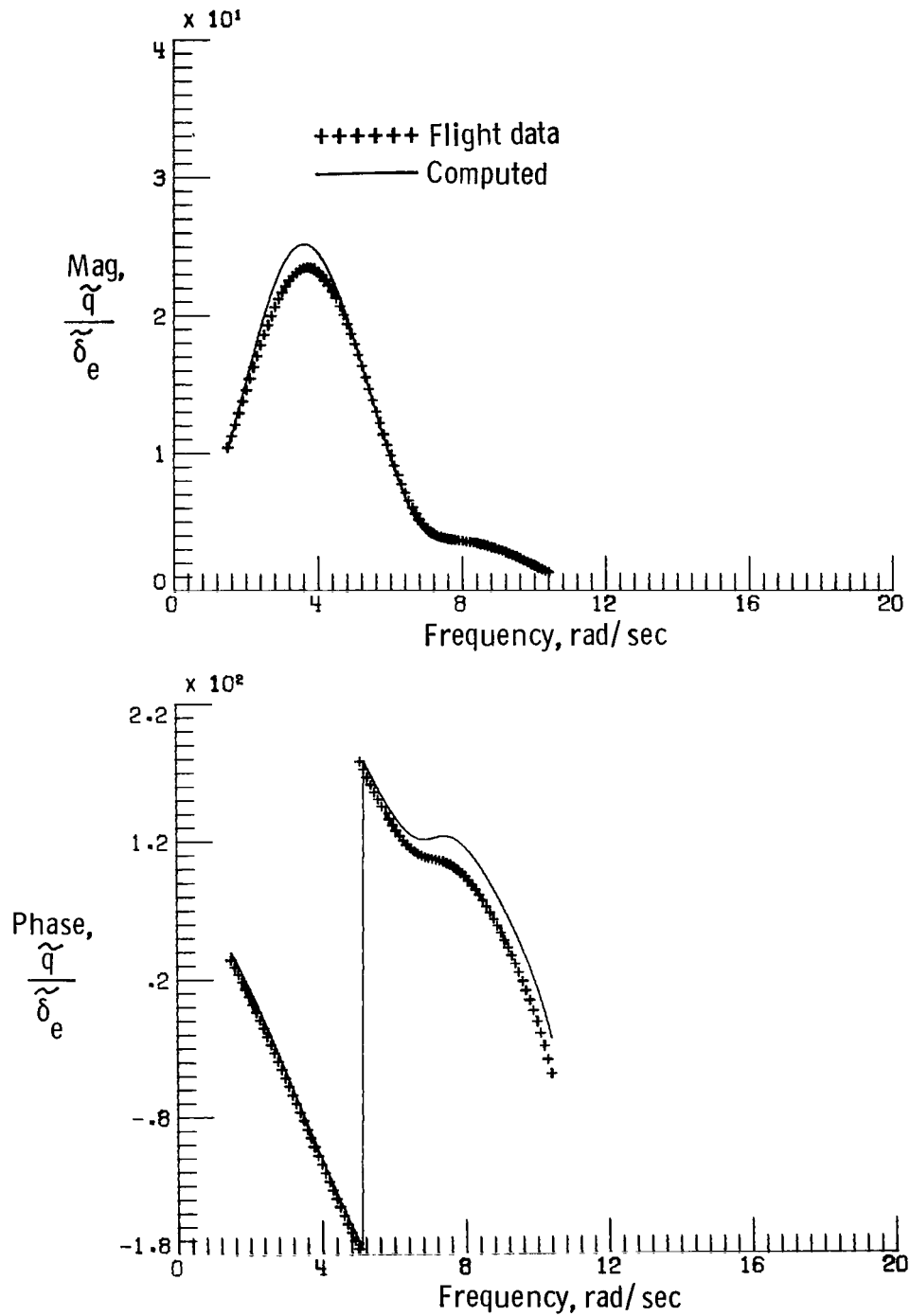
(c) Normal-acceleration response.

Figure 6.- Concluded.



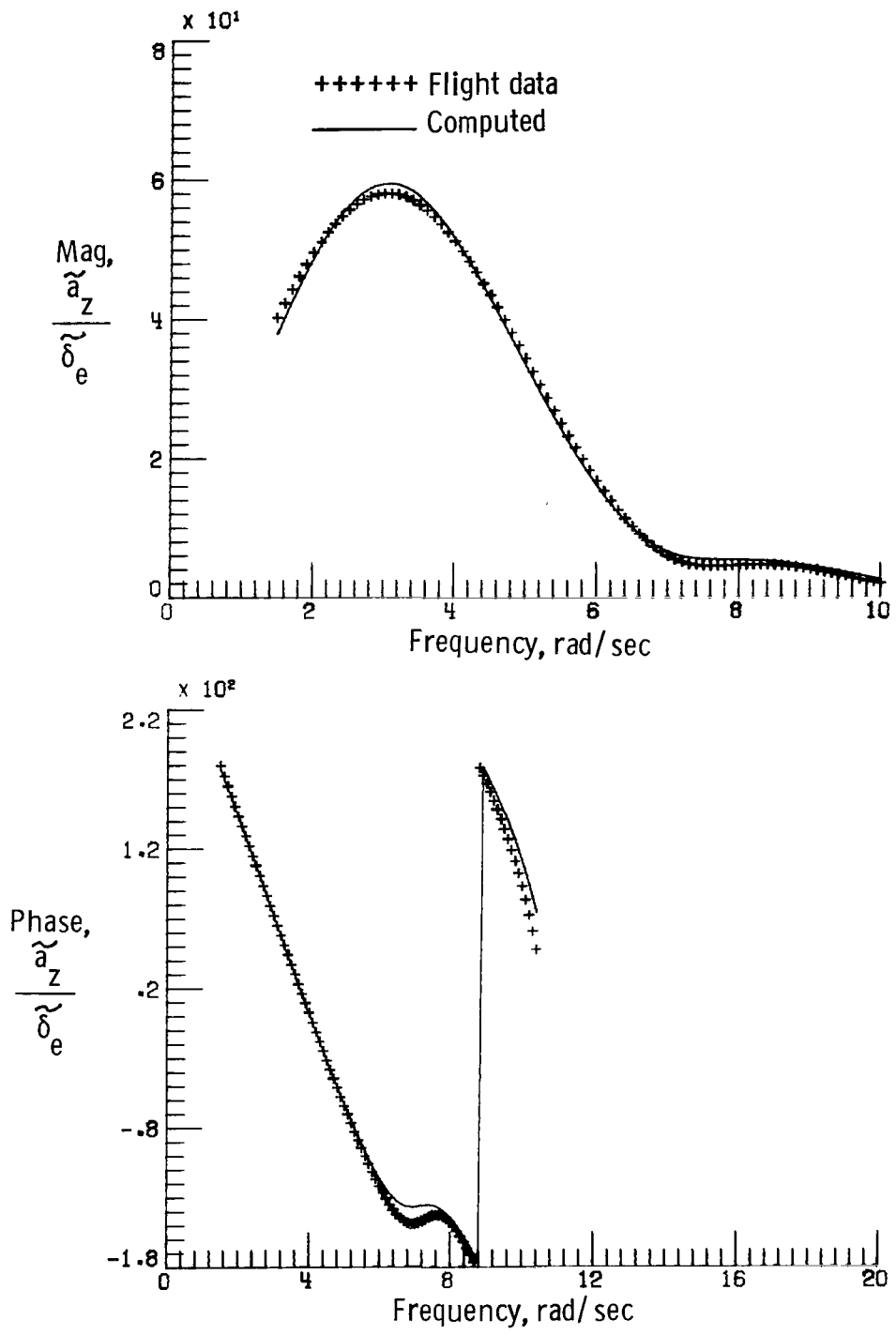
(a) Angle-of-attack response.

Figure 7.- Flight test data in frequency domain and data computed using extracted parameters when extraction algorithm neglected unsteady aerodynamics.



(b) Pitch-rate response.

Figure 7.- Continued.



(c) Normal-acceleration response.

Figure 7.- Concluded.

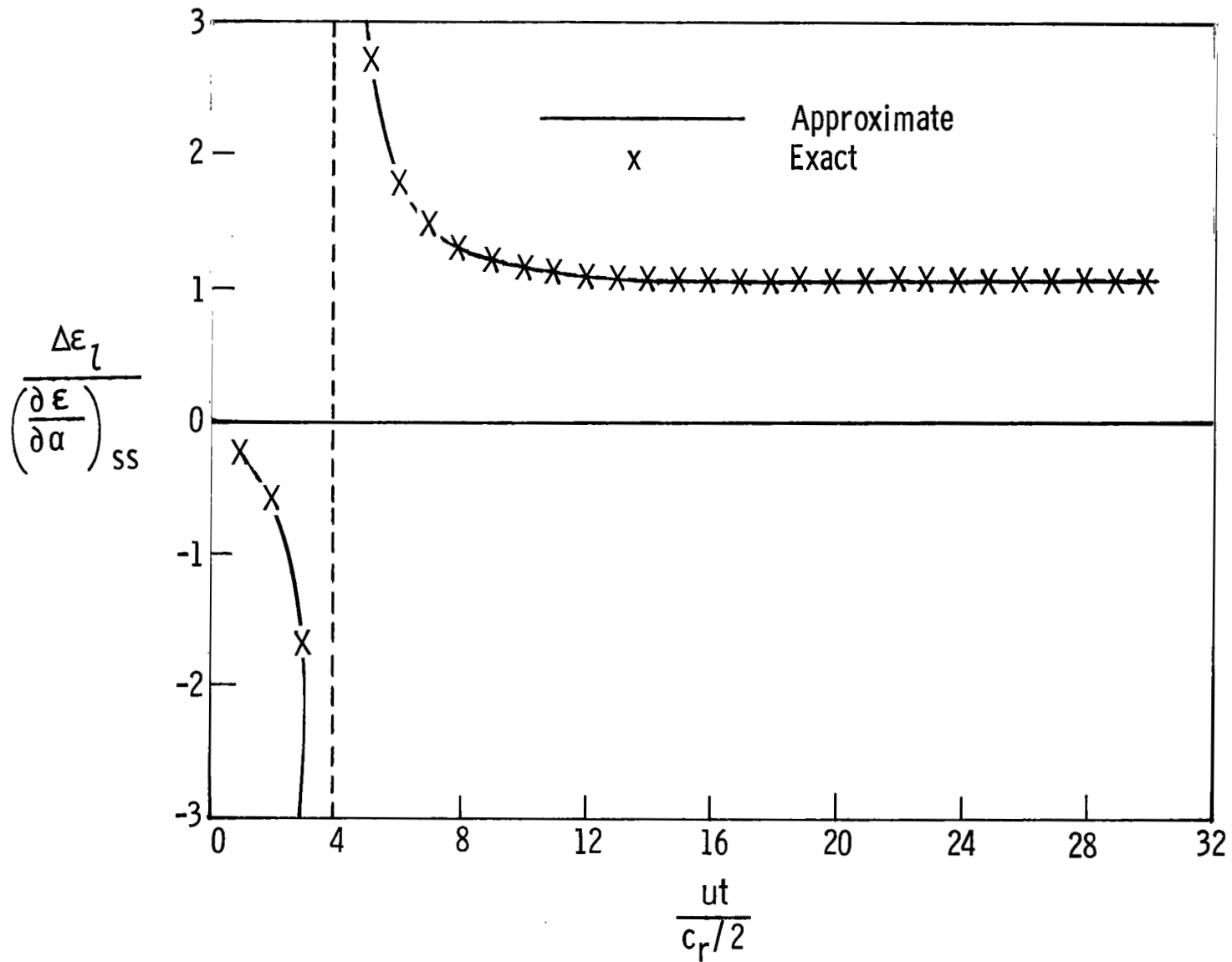
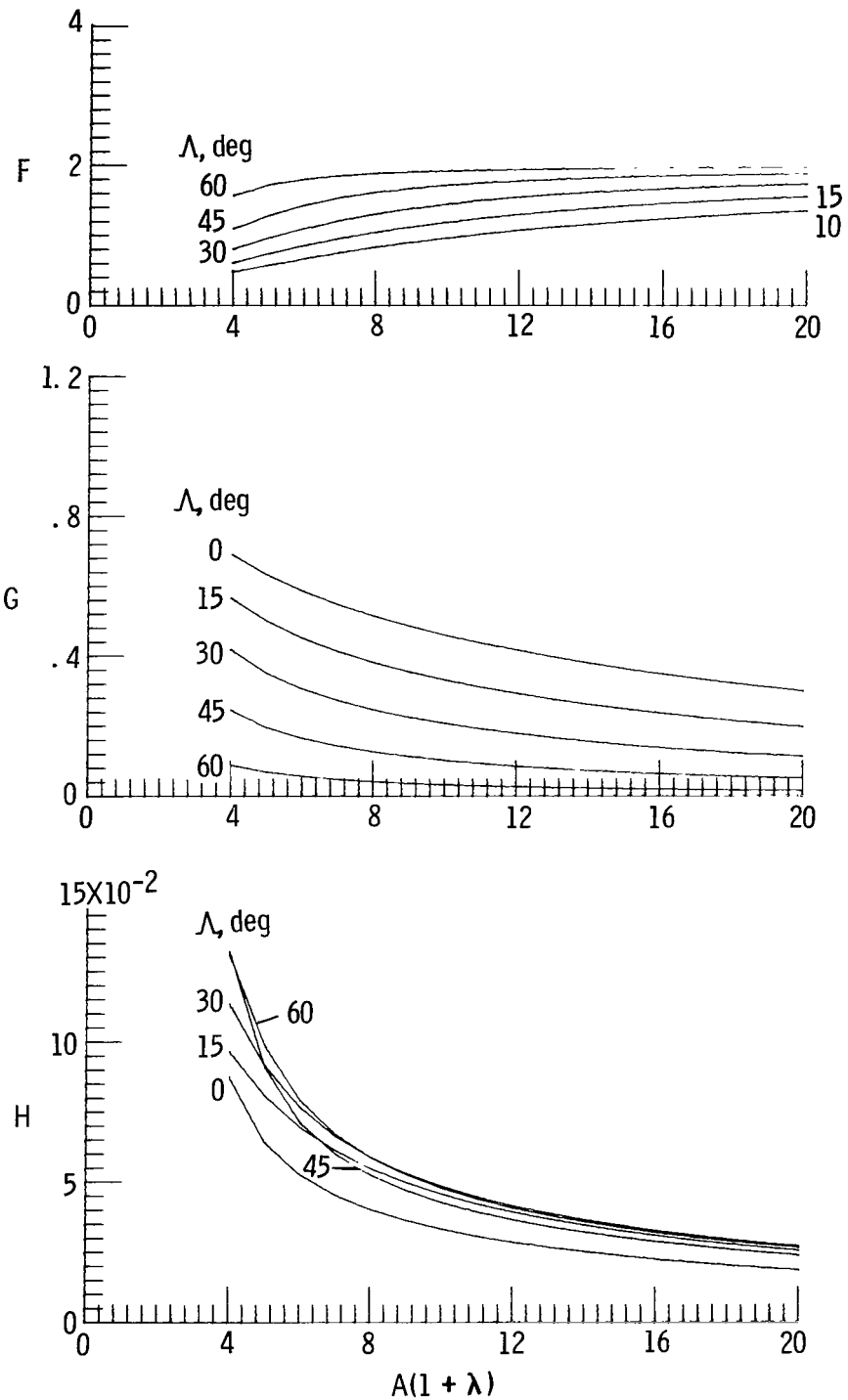
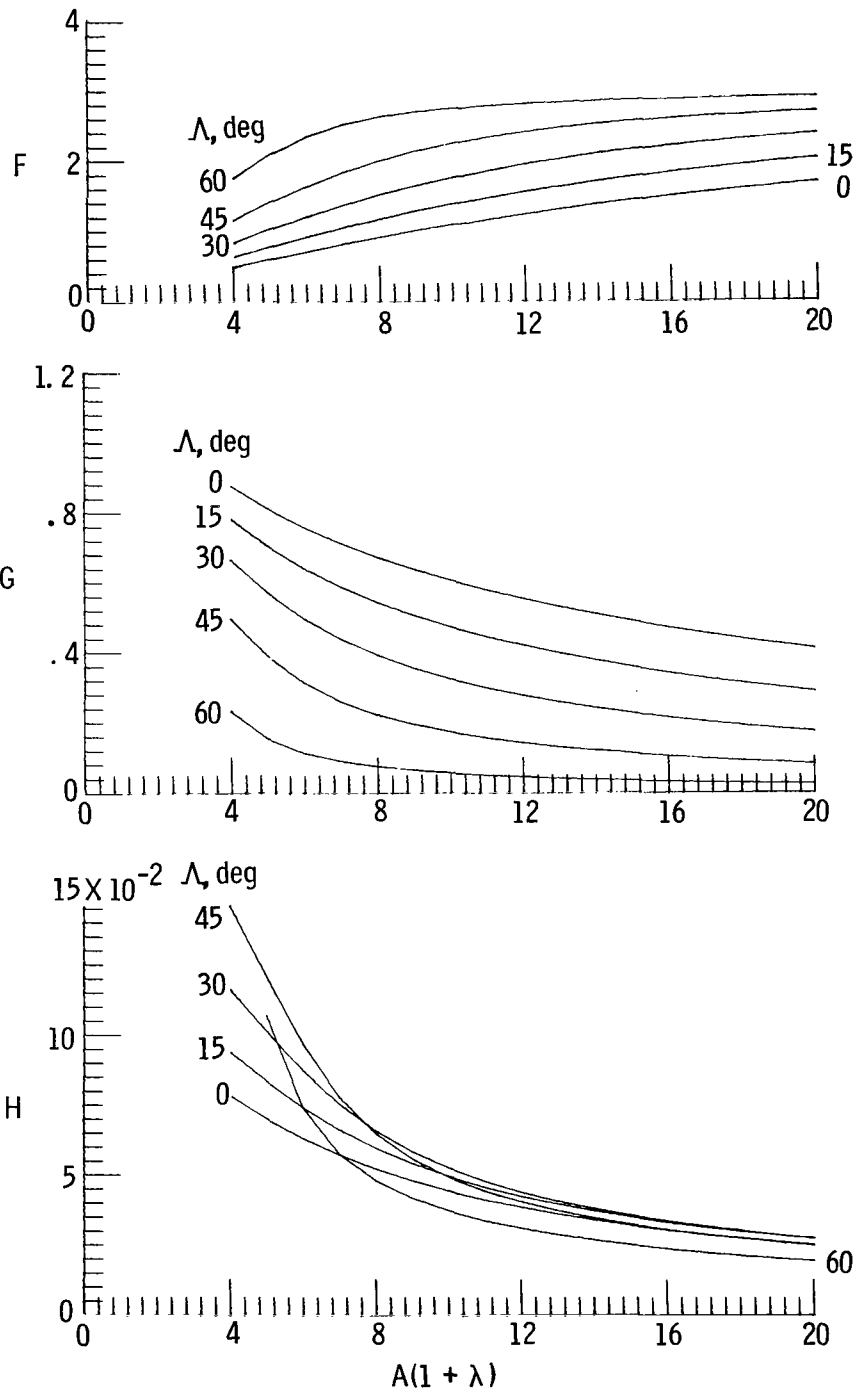


Figure 8.- Comparison of results from exact and approximate downwash equations.



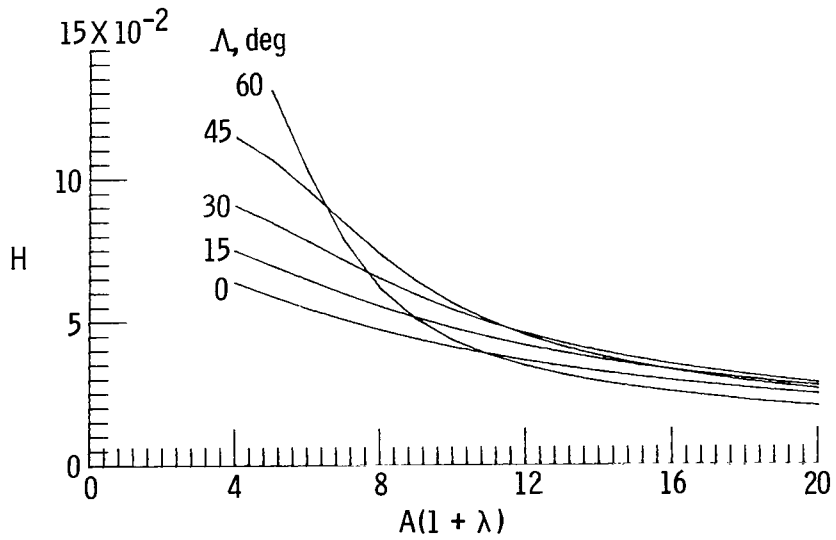
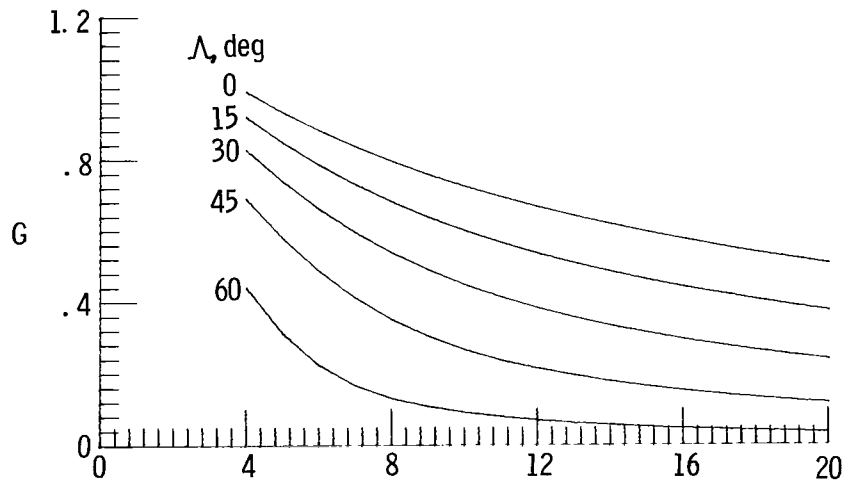
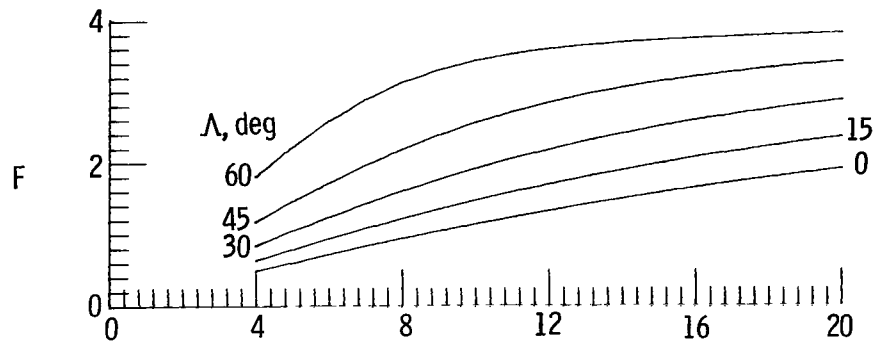
(a) $\frac{\lambda}{c} = 2.$

Figure 9.- Values of constants F, G, and H for use in downwash calculations.



(b) $\frac{l}{c} = 3.$

Figure 9.- Continued.



(c) $\frac{\lambda}{c} = 4.$

Figure 9.- Concluded.

1. Report No. NASA TP-1536		2. Government Accession No.		3. Recipient's Catalog No.	
4. Title and Subtitle INCLUSION OF UNSTEADY AERODYNAMICS IN LONGITUDINAL PARAMETER ESTIMATION FROM FLIGHT DATA				5. Report Date December 1979	
7. Author(s) M. J. Queijo, William R. Wells, and Dinesh A. Keskar				6. Performing Organization Code	
9. Performing Organization Name and Address NASA Langley Research Center Hampton, VA 23665				8. Performing Organization Report No. L-13009	
12. Sponsoring Agency Name and Address National Aeronautics and Space Administration Washington, DC 20546				10. Work Unit No. 505-34-33-06	
15. Supplementary Notes M. J. Queijo: Langley Research Center, Hampton, Virginia. William R. Wells: Wright State University, Dayton, Ohio. Dinesh A. Keskar: SDC Integrated Services, Hampton, Virginia.				11. Contract or Grant No.	
16. Abstract <p>A simple vortex system is used to model unsteady aerodynamic effects into the rigid-body longitudinal equations of motion of an aircraft. With the formulation used, only steady-state aerodynamic derivatives appear in the equations. It is found expedient to transform the equations into the frequency domain to make them useful for extracting aerodynamic parameters from flight data. The equations are used in the development of a parameter-extraction algorithm. If the algorithm is used with the unsteady aerodynamic modeling included, all extracted aerodynamic derivatives are the steady-state derivatives. If unsteady aerodynamic modeling is omitted, some extracted parameters include the effects of unsteady aerodynamics and are interpreted as combinations of steady-state and acceleration parameters. Use of the two parameter-estimation modes, one including and the other omitting unsteady-aerodynamic modeling, provides a means of estimating some acceleration derivatives. Computer-generated data and flight data are used to demonstrate the use of the parameter-extraction algorithm.</p>				13. Type of Report and Period Covered Technical Paper	
17. Key Words (Suggested by Author(s)) Unsteady aerodynamics Parameter identification				14. Sponsoring Agency Code	
18. Distribution Statement Unclassified - Unlimited				Subject Category 02	
19. Security Classif. (of this report) Unclassified		20. Security Classif. (of this page) Unclassified		21. No. of Pages 50	
				22. Price* \$4.50	

* For sale by the National Technical Information Service, Springfield, Virginia 22161

NASA-Langley, 1979

National Aeronautics and
Space Administration

Washington, D.C.
20546

Official Business

Penalty for Private Use, \$300

THIRD-CLASS BULK RATE

Postage and Fees Paid
National Aeronautics and
Space Administration
NASA-451



1 1 1U,A, 121179 S00903DS
DEPT OF THE AIR FORCE
AF WEAPONS LABORATORY
ATTN: TECHNICAL LIBRARY (SUL)
KIRTLAND AFB NM 87117

NASA

POSTMASTER: If Undeliverable (Section 158
Postal Manual) Do Not Return
